Unifying Sensitivity Estimates to Heavy Neutral Leptons at Current and Near Future Experiments

Reisinger, Tim

Unifying Sensitivity Estimates to Heavy Neutral Leptons at Current and Near Future Experiments

Thesis

submitted in partial fulfillment of the
requirements for the degree of

Master Of Science
in
Physics

Author :	T. Reisinger
Student ID :	s1838962
Supervisor :	Prof. A. Boyarsky
Second corrector :	Prof.dr. K.E. Schalm

Leiden, The Netherlands, August 9, 2023

Unifying Sensitivity Estimates to Heavy Neutral Leptons at Current and Near Future Experiments

T. Reisinger

Huygens-Kamerlingh Onnes Laboratory, Leiden University
P.O. Box 9500, 2300 RA Leiden, The Netherlands

August 9, 2023

Abstract

The three pressing problems in modern particle physics, neutrino mass, baryon asymmetry and dark matter inspired various models among which many new particles and experiments to either verify or exclude their existence. Among the most promising examples is the right handed neutrino or heavy neutral lepton (HNL) that has the potential to deal with all the beyond standard model (BSM) physics at once. We use fairly simple and robust pseudo-analytical methods to calculate the sensitivities of various proposed or already running BSM focused experiments among which extracted beamline experiments at CERN (SHiP, SHADOWS and NA62 DUMP), collider experiments at the LHC (MATHUSLA, Codex-b, FASER2 and FACET) and the DUNE ND detector at Fermilab. We found good agreement with sensitivities in the literature, provided a consistent way to compare different experiments and a fast and flexible way of calculating sensitivities that allows for quick adjustment in case of design changes or other developments in the field.

Contents

1 Introduction **7**
- 1.1 Neutrino Oscillations 8
  - 1.1.1 Neutrino Mass 8
  - 1.1.2 Neutrino Oscillation 12
- 1.2 Baryon Asymmetry 14
- 1.3 Dark Matter 17
- 1.4 Portals 19
- 1.5 Outline of this Thesis 20

2 Heavy Neutral Leptons **23**
- 2.1 The Seesaw Mechanism 24
- 2.2 HNL Production 26
- 2.3 HNL Decay 27

3 Experimental Searches for HNLs **31**
- 3.1 Extracted Beam Lines at CERN 31
  - 3.1.1 SHiP 32
  - 3.1.2 NA62 32
  - 3.1.3 SHADOWS 33
- 3.2 LHC based Experiments 33
  - 3.2.1 MATHUSLA 34
  - 3.2.2 Codex-b 34
  - 3.2.3 FASER 34
  - 3.2.4 FACET 35
- 3.3 DUNE ND 36

4 Sensitivities of Experiments **39**
- 4.1 How to Calculate the Sensitivity of an Experiment 40

4.2 Upper and Lower Boundaries of Sensitivity Curves 44
4.3 Distribution Functions 44
4.3.1 Distribution function of extracted beamline experiments 45
4.3.2 Distribution of D and B mesons at the LHC 46
4.3.3 Distribution of D mesons at DUNE 46

5 Results 49
5.1 Results for Beam Dump Experiments at CERN 49
5.2 Results for LHC Based Experiments 50
5.3 Results for DUNE ND 50
5.4 Comparison to Literature 52
5.4.1 Comparing the extracted beam lines at CERN 52
5.4.2 Comparing results for the LHC based experiments 52
5.4.3 Comparing the DUNE ND result 54

6 Conclusions 55

Chapter 1

Introduction

Even though the Standard Model (SM) is self-consistent and describes our perceivable physical reality with exceptional accuracy, already before and also after its formulation, experimental evidence had been gathered that betrays the incompleteness of the theory when it comes to describing all the fundamental particles and their interactions. The field of theoretical particle physics has therefore been occupied to account for these inconsistencies between theory and experiment both within the framework of quantum field theory, the theory upon which the Standard Model is based, and beyond.
The three well known beyond Standard Model (BSM) phenomena that show this incompleteness are:

1. Neutrino oscillation

2. Baryon asymmetry

3. Dark matter

We will give a short overview of these problems in the coming sections.
Many efforts are under way to validate or exclude many BSM models that have so far been proposed and since these models are so plentiful, the emphasis rests on the word exclude. In this thesis we will look at such efforts in the form of elaborate experiments primarily at CERN and investigate their ability to probe these models. In particular we will look at so called right heavy neutral leptons (HNLs) also known as right handed or sterile neutrinos which have the potential to solve all the BSM phenomena at once.

1.1 Neutrino Oscillations

Neutrino's appearing to changing their flavour, also called neutrino oscillation, was first proposed by Bruno Pontecorvo in 1957 analogous to neutral kaon mixing [1]. Roughly ten years later the first experimental evidence for neutrino oscillations, although then not conclusively linked to it, was found in the form of an apparent deficit in solar neutrino's that later became known as the solar neutrino problem [2]. Since neutrino's interact so weakly, experimental research was difficult and only in the late 90's the first strong evidence for neutrino oscillation was obtained in the Super-Kamiokande observatory in Japan [3].

1.1.1 Neutrino Mass

The fact that neutrino's oscillate means that their mass is nonzero. The Standard Model however, neutrino masses are strictly zero. The observation of neutrino oscillations thus proves the incompleteness of our current standard model as a means of describing all present fundamental particles and their interactions. In this section we will outline the relevant theoretical background of the neutrino mass and explain why it does not appear in the standard model. To illustrate why it is nontrivial for neutrinos to have mass we look at the Dirac equation:

$$(i\gamma^\mu \partial_\mu - m)\psi(x) = 0. \tag{1.1}$$

In the chiral or Weyl basis $\psi(x)$ can be written as:

$$\psi(x) = \begin{bmatrix} \xi_L \\ \xi_R \end{bmatrix} \tag{1.2}$$

Where ξ_L and ξ_R are the left and right chirality states respectively. These states transform into each other under the parity transformation $P : \vec{x} \to -\vec{x}$, just like any other chiral object. The γ^μ matrices in this basis look like:

$$\gamma^0 = \begin{bmatrix} 0 & I_2 \\ I_2 & 0 \end{bmatrix}, \qquad \gamma^i = \begin{bmatrix} 0 & \sigma^i \\ -\sigma^i & 0 \end{bmatrix} \qquad \gamma^5 = \begin{bmatrix} -I_2 & 0 \\ 0 & I_2 \end{bmatrix}. \tag{1.3}$$

Where $\gamma^5 = i\gamma^0\gamma^1\gamma^2\gamma^3$. We can use this matrix to construct an operator that projects an arbitrary state onto its left or right chiral eigenstates and is given by:

$$P_L = \frac{1-\gamma^5}{2}, \qquad P_R = \frac{1+\gamma^5}{2} \tag{1.4}$$

We define:

$$\psi_L \equiv P_L\psi = \begin{bmatrix} \xi_L \\ 0 \end{bmatrix}, \qquad \psi_R \equiv P_R\psi = \begin{bmatrix} 0 \\ \xi_R \end{bmatrix}. \tag{1.5}$$

We can now decompose the Dirac equation in two separate equations:

$$\begin{bmatrix} -m & i\sigma_\mu\partial^\mu \\ i\bar{\sigma}_\mu\partial^\mu & -m \end{bmatrix} \begin{bmatrix} \xi_L \\ \xi_R \end{bmatrix} = 0, \qquad (\sigma_\mu := (1, \boldsymbol{\sigma}) \text{ and } \bar{\sigma}_\mu := (1, -\boldsymbol{\sigma})). \tag{1.6}$$

Where $\boldsymbol{\sigma}$ is the vector of Pauli matrices. Multiplying this out and rearranging we see that the right-handed and left-handed spinors couple or "mix":

$$\begin{bmatrix} i\sigma_\mu\partial^\mu\xi_R \\ i\bar{\sigma}_\mu\partial^\mu\xi_L \end{bmatrix} = \begin{bmatrix} m\xi_L \\ m\xi_R \end{bmatrix} \tag{1.7}$$

This is because otherwise the equation is not Lorentz covariant. It is therefore necessary when trying to construct a Lorentz invariant mass term in the Lagrangian for a massive fermion, that in the mass term the left and right handed parts of $\psi(x)$ also mix. This can be achieved by writing the mass term as:

$$\mathcal{L}_{\text{fermion mass}} = -m\psi^\dagger\gamma^0\psi = -m(\psi_L^\dagger+\psi_R^\dagger)\gamma^0(\psi_L+\psi_R) = -m(\psi_R^\dagger\psi_L+\psi_L^\dagger\psi_R) \tag{1.8}$$

Where $\psi^\dagger\gamma^0$ is often written as $\bar{\psi}$, this is known as the Dirac conjugate. Now since neutrinos are massive, one would expect the neutrino mass term to look something like eq. 1.8. But unfortunately since the 1957 experiment by Wu et al.[4] we know that only left-handed neutrinos and right-handed **anti**neutrinos are observed so such a mass term cannot be written.

Let us try to find a suitable mass term for the neutrino. For our current discussion it is important to introduce the charge conjugation operator C. Multiplied by the transpose of the Dirac conjugate of the fermion field, it describes a particle of opposite charge and thus its antiparticle. We denote it as:

$$\psi^c \equiv C\bar{\psi}^T \tag{1.9}$$

This fermion field also satisfies the Dirac equation. The charge conjugation operator C has the following useful properties:

$$C\gamma^{\mu T} = -\gamma^\mu C, \qquad C\gamma^{5T} = \gamma^5 C, \qquad C^T = -C = C^{-1} = C^\dagger. \tag{1.10}$$

Let us try to write a mass term that only includes left handed neutrinos. A good first attempt is to consider neutrinos as Majorana fermions. Ettore Majorana discovered a fully imaginary representation of the gamma matrices. This means that the coefficients in the Dirac equation are all real. Solutions ψ to the Dirac equation are thus real:

$$\psi^* = \psi. \tag{1.11}$$

The γ matrices in the Majorana basis look like:

$$\gamma^0_M = \begin{bmatrix} 0 & \sigma^2 \\ \sigma^2 & 0 \end{bmatrix}, \qquad \gamma^1_M = i \begin{bmatrix} \sigma^3 & 0 \\ 0 & \sigma^3 \end{bmatrix}, \qquad \gamma^2_M = \begin{bmatrix} 0 & -\sigma^2 \\ \sigma^2 & 0 \end{bmatrix}, \qquad \gamma^3_M = -i \begin{bmatrix} \sigma^1 & 0 \\ 0 & \sigma^1 \end{bmatrix}. \tag{1.12}$$

The matrix C in the Majorana representation can by found by imposing it must satisfy the relations of eq.1.10 and is found to be:

$$C_M = -\gamma^0_M = -\begin{bmatrix} 0 & \sigma^2 \\ \sigma^2 & 0 \end{bmatrix}. \tag{1.13}$$

We can now see that charge conjugation corresponds to complex conjugation of the fermion field in the Majorana basis:

$$\psi^c = C(\psi^\dagger \gamma^0_M)^T = C(\gamma^0_M)^T \psi^* = (-\gamma^0_M)(-\gamma^0_M)\psi^* = \psi^* \tag{1.14}$$

Where we used that γ^0_M is anti-symmetric, hermitian and squares to the identity. Since a Majorana fermion is real valued, complex conjugation and thus charge conjugation leaves the state the same. This means that these Majorana fermions are neutrally charged and are therefore their own antiparticles. A fermion being its own anti particle can in general be written like this:

$$\psi^c = \psi \tag{1.15}$$

This is sometimes called the Majorana condition. This condition imposes extra constraints which result in the Majorana fermion having only two degrees of freedom. Another way this can be seen is by looking at how the charge conjugation acts on the individual chiral components of a Majorana spinor field ψ. We can write ψ as a linear combination of its chiral eigenstates:

$$\psi = \psi_L + \psi_R \tag{1.16}$$

Since $\psi^c = \psi$:

$$\psi = \psi_L + (\psi^c)_R \tag{1.17}$$

We now compute the last term on the right hand side:

$$(\psi^c)_R = \frac{1+\gamma^5}{2} C \bar{\psi}^T = \frac{1+\gamma^5}{2} C(\psi^\dagger \gamma^0)^T = \frac{1+\gamma^5}{2} C(\gamma^0)^T (\psi^\dagger)^T \tag{1.18}$$

Using the relations from eq. 1.10 we can rewrite further:

$$\begin{aligned}(\psi^c)_R &= -\frac{1+\gamma^5}{2}\gamma^0 C(\psi^\dagger)^T \\ &= -\gamma^0\frac{1-\gamma^5}{2}C(\psi^\dagger)^T \\ &= -\gamma^0 C\frac{1-(\gamma^5)^T}{2}(\psi^\dagger)^T \\ &= C(\gamma^0)^T P_L^T\psi^\dagger)^T \\ &= C(\psi^\dagger P_L^\dagger\gamma^0)^T \\ &= C((P_L\psi)^\dagger\gamma^0)^T \\ &= C\bar{\psi_L}^T = (\psi_L)^c\end{aligned}$$

Where we have used in the second line that $\{\gamma^5, \gamma^\mu\} = 0$ and that P_L is hermitian in the fifth line. We can thus conclude that acting on a chiral field with the charge conjugation operation flips its chirality and in the case of a Majorana fermion field that it can be entirely constructed out of one chirality state:

$$\psi = \psi_L + (\psi^c)_R = \psi_L + (\psi_L)^c \tag{1.19}$$

This means that the Majorana fermion has only two degrees of freedom (instead of four for the Dirac fermion). We now want to write a Majorana mass term for the Lagrangian. Let us construct a term quadratic in the field like in eq. 1.8:

$$\begin{aligned}\bar{\psi}\psi &= \overline{(\psi_L+\psi_R)}(\psi_L+\psi_R) \\ &= \overline{(\psi_L+\psi_L^c)}(\psi_L+\psi_L^c) \\ &= \bar{\psi}_L\psi_L + \bar{\psi}_L\psi_L^c + \bar{\psi}_L^c\psi_L + \bar{\psi}_L^c\psi_L^c \\ &= \bar{\psi}_L\psi_L^c + \bar{\psi}_L^c\psi_L\end{aligned}$$

The Majorana mass term looks like:

$$\mathcal{L}_{\text{Majorana mass}} = -\frac{1}{2}m(\bar{\psi}_L\psi_L^c + \bar{\psi}_L^c\psi_L) \tag{1.20}$$

Where the factor of $\frac{1}{2}$ comes from the fact that the term is quadratic in ψ_L. One important detail about this mass term is that it violates lepton dumber ($\Delta L = 2$). This fact can be exploited to look proof or disprove the Majorana nature of neutrinos by looking for lepton number violating processes like neutrinoless double β-decay.
We now have a possible explanation for neutrino masses but the only problem is that weak symmetry mixes neutrinos with their corresponding charged lepton.

This will result in a Majorana mass for the charged leptons as well but a Majorana particle cannot have charge!

The way to resolve this is to let the Majorana term arise from a spontaneously broken term known as the Weinberg dimension-5 operator[5]. It looks like:

$$\mathcal{O}_W = \frac{c_{\alpha\beta}}{\Lambda}\bar{L}^c_\alpha \tilde{H}^* \tilde{H}^\dagger L_\beta + h.c. \tag{1.21}$$

Where $\tilde{H} = i\sigma^2 H^*$. After electroweak symmetry breaking this operator leads to a Majorana mass for the neutrino's. The factor of $1/\Lambda$ suppresses the operator so that it only becomes relevant at energies $\approx \Lambda$. Assuming $c_{\alpha\beta} \sim \mathcal{O}(1)$:

$$\Lambda \sim \frac{v^2}{m_L} \sim 10^{15} GeV \tag{1.22}$$

Where v is the vacuum expectation value (VEV) of the Higgs field. Assuming a sub eV mass for the neutrino ($\sum m_\nu < 0.12$ eV [6]). These kinds of operators suggest that the standard model Lagrangian $\mathcal{L}_{sm}$ is a theory only effective at low energies and that new physics is hidden at higher energy scales shown by effective higher dimensional operators. The Weinberg operator is not unique, it is merely the lowest $d > 4$ dimensional operator using only standard model fields thus making it a good effective theory for the neutrino mass.

Another way to give the neutrino mass is to introduce a new particle, a right handed neutrino typically written as N. This is a standard model gauge singlet that is allowed a Yukawa interaction with the leptonic doublet L_α and the Higgs doublet $\tilde{H}$:

$$\mathcal{L}_y = -F_\alpha \bar{L}_\alpha \tilde{H} N + h.c. \tag{1.23}$$

Upon electroweak symmetry breaking a Dirac mass term emerges:

$$\mathcal{L}_y \xrightarrow{\langle \tilde{H} \rangle \neq 0} \frac{v}{\sqrt{2}} y_v \bar{\nu}_L N + h.c. \tag{1.24}$$

1.1.2 Neutrino Oscillation

We finally have a theory for the neutrino mass but it might not be immediately obvious how flavour oscillations require mass. A somewhat intuitive explanation might be that massless particles travel at the speed of light, and according to special relativity time goes infinitely slow for objects traveling at light speed so it is impossible to observe any change in the properties of the particle. This however does not tell us anything quantitative. So lets approach this phenomenon a little more formal and quantum mechanical to see what is really going on.

Neutrino oscillations essentially arise because weak interactions conserve lepton flavour, but the energy (or mass) eigenstates of neutrinos $|\nu_i\rangle$ are not flavour eigenstates $|\nu_i\rangle$. This leads to the flavour eigenstates mismatching with the mass eigenstates. But of course since the eigenstates of observables always form an orthonormal basis we can write one state in terms of the other. For the electron neutrino this looks like:

$$|\nu_e\rangle = U_{1e}^* |\nu_1\rangle + U_{2e}^* |\nu_2\rangle + U_{3e}^* |\nu_3\rangle . \tag{1.25}$$

Where U_{ie}^* are elements of the PMNS (Pontecorvo-Maki-Nakagawa-Sakata [7]) matrix U and quantifies the mixing of the three known neutrinos. To derive oscillations, people usually consider a wave packet of 3 mass eigenstates with some fixed common momenta and different energies. While this leads to the correct result, the derivation has to be performed more accurately by considering the density matrix of all particles that are created with the neutrino. For more details on this see [8]. We present the illustrative derivation:

$$|\nu_\alpha\rangle = \sum_i U_{\alpha i}^* |\nu_i\rangle , \tag{1.26}$$

where $\alpha = e, \mu, \tau$ label the flavour eigenstates and $i = 1, 2, 3$ the mass eigenstates. In a vacuum each mass eigenstate evolves with a phase factor of $e^{-iE_i t}$, this gives:

$$|\nu_\alpha(t)\rangle = \sum_i U_{\alpha i}^* e^{-iE_i t} |\nu_i\rangle . \tag{1.27}$$

Where E_i is the relativistic energy $\sqrt{p^2 + m_i^2}$ and we define $|\nu_\alpha(t=0)\rangle := |\nu_\alpha\rangle$. The probability to find a neutrino initially in state α at a certain time t in state β is:

$$P(\nu_\alpha \to \nu_\beta) = |\langle \nu_\beta | \nu_\alpha(t) \rangle|^2 = \left| \sum_i U_{\beta i} U_{\alpha i}^* e^{-iE_i t} \right|^2 . \tag{1.28}$$

We can simplify the exponent upon noticing that the neutrino's are ultra relativistic. That means that their mass is very small compared to their momentum. We can therefore approximate the energy as $E_i = \sqrt{p^2 + m_i^2} \approx p + \frac{m_i^2}{2p} \approx E + \frac{m_i^2}{2E}$ since $p \approx E$ where E is the energy of the wave packet. After dropping the phase e^{-iEt}, this expression can be rewritten as:

$$\begin{aligned} P(\nu_\alpha \to \nu_\beta) = \delta_{\alpha\beta} &- 4 \sum_{i<j} Re(U_{\alpha i} U_{\beta i}^* U_{\alpha j}^* U_{\beta j}) \sin^2 \left(\frac{\Delta m_{ji}^2 L}{4E} \right) \\ &+ 2 \sum_{i<j} Im(U_{\alpha i} U_{\beta i}^* U_{\alpha j}^* U_{\beta j}) \sin \left(\frac{\Delta m_{ji}^2 L}{4E} \right), \end{aligned} \tag{1.29}$$

Version of August 9, 2023– Created August 9, 2023 - 19:58

where Δm^2_{ji} is the mass squared difference $m^2_j - m^2_i$ and $L \approx ct$. This formula characterises the oscillation behaviour of the three (anti-)neutrino flavours. For anti neutrino oscillation you need to replace $U \to U^*$ in eq. 1.29. Equation 1.29 also gives us another piece of information about neutrino masses, namely that in order for neutrinos to oscillate, not only do they need to be massive, but their masses also need to be non-degenerate $m_i \neq m_j$. This is obvious, since if the masses are equal, you can define the mass basis however you like, along the flavour eigenstates for example.
One might be inclined to think that there is no reason to believe that charged leptons might not be able to oscillate as well. In a way they do, but the effect is so negligible that in practically all cases the effect can be ignored. If the production of more than one lepton flavour is allowed in a certain weak process, the states produced are either produced in a incoherent state or the state loses its coherence very quickly within a microscopic distance due to the extreme mass difference between the charged leptons. Oscillations of charged leptons would only be observable at extremely high energies that are off limits for contemporary experiments. For further details see [9].

1.2 Baryon Asymmetry

Observations suggest that there is a significant asymmetry between baryons (protons and neutrons) and antibaryons (antiprotons and antineutrons). As far as we can tell there are no stars, planets or galaxies made entirely from antimatter. The baryon asymmetry can be quantitatively characterized as follows:

$$\eta = \left.\frac{n_B - n_{\bar{B}}}{n_\gamma}\right|_{t=0} \approx 6.21 \cdot 10^{-10}. \tag{1.30}$$

The average number density in the universe of the baryons and antibaryons is here n_B and $n_{\bar{B}}$ respectively and n_γ is the relic photon number density. Various considerations highly suggest that baryon asymmetry came about dynamically and was therefore not an "initial condition" of the universe. For example, assuming inflation happened, it would have diluted away most of the baryon asymmetry. A dynamical process resulting in baryon asymmetry is called baryogenesis. For baryogenesis to occur three conditions must be satisfied. These are called the Sakharov conditions [10]:

1. **Baryon number violation**. In order for the asymmetry to arise from an initial state where there is no asymmetry, baryon number must be violated. There are processes using only standard model physics that seem to violate

baryon number due to the chiral anomaly or Adler-Bell-Jackiw anomaly [11]. This is a process that arises from quantum corrections to the classical axial current resulting from the global symmetry transformation for each of the twelve fermionic fields:

$$\psi_L^i \to e^{i\beta}\psi_L^i \Rightarrow j_i^\mu = \overline{\psi}^i \gamma^\mu \psi^i. \tag{1.31}$$

In the classical theory these currents are conserved but upon quantizing the theory so called anomalies arise in the one loop level. This correction leads to the current to be not conserved:

$$\partial_\mu j_i^\mu = \frac{1}{64\pi} F^A_{\mu\nu} \tilde{F}^{\mu\nu A}, \qquad \tilde{F}^{\mu\nu} = \frac{1}{2}\epsilon^{\mu\nu\alpha\beta} F^A_{\alpha\beta} \tag{1.32}$$

Gauge field configurations where $\int F\tilde{F}dx^4 \neq 0$ are called instantons. These are finite action classical solutions to the unquantized field theory in Euclidean spacetime. And describes tunneling between different vacua with different winding numbers. This winding number (or Chern-Simons) number of a particular field configuration is obtained upon integrating the right hand side over all spacetime and is related to it's topology. For more information on this topic see [12]. The left hand term gives the total difference in charge:

$$\Delta Q^i = Q^i(t=-\infty) - Q^i(t=\infty) = \int \partial_\mu j_i^\mu dx^4 = \frac{1}{64\pi}\int F^A_{\mu\nu}\tilde{F}^{\mu\nu A} dx^4 \in \mathbb{Z}. \tag{1.33}$$

Imagining a ground state of our gauge field as a periodic potential where each minimum labelled by a different winding numbers, instantons are the vacuum fluctuations that tunnel between these minima. However you can also climb over the potential barrier given a high enough energy. The configuration mediating this process is called a sphaleron. The sphaleron (Greek for "slippery thing") is an unstable static solution to the electroweak field equations that are saddle points in infinite dimensional field space which separate two local minima or vacua and corresponds to half integer winding numbers. Going from one vacuum to the other takes a lot of energy ($\approx$ 9TeV) and leads different winding numbers and therefore a different number of fermions or anti fermions. This process would either convert three baryons into three antileptons or three antibaryons into three leptons (or vice versa). This process violates B+L current but still conserves B-L current through the above described Adler-Bell-Jackiw anomaly.
In summary, for low temperatures B+L current can be violated via the tunneling from one winding number to the other via instanton process and for

high temperatures the potential barrier can be overcome by the sphaleron. The tunneling probability of the instanton is suppressed by the instanton action and therefore exceptionally small and will hardly contribute to the baryon asymmetry [11]. The transition rate is:

$$\Gamma_{instanton} \propto e^{-\frac{8\pi^2}{g^2}} \sim 10^{-82}. \tag{1.34}$$

Where $g \approx 0.65$ is the coupling constant present in the electroweak theory of the standard model. For the sphaleron in the presence of a non zero vacuum expectation value (VEV) of the Higgs field the transition rate is Boltzmann suppressed and goes like:

$$\Gamma_{sphaleron} \propto e^{-\frac{E_{sph}}{T}} \qquad (E_{sph} \approx 9 \text{ TeV}). \tag{1.35}$$

We are however interested in the rate before the electroweak symmetry breaking occurred due to the electroweak phase transition (EWPT) where the VEV of the Higgs field was zero. In this regime the sphaleron transition rate is no longer suppressed by a Boltzmann factor and is estimated to be [13]:

$$\Gamma_{B+L\ violation} \approx 25\alpha_W^5 T^4 \tag{1.36}$$

Where $\alpha_W = \alpha / \sin\theta_W$ with α the fine structure constant. We can conclude that before the EWPT the $B + L$ current could have been violated and thus satisfy the first Sakharov condition.

2. **C and CP violation**. If either C or CP were conserved, then processes involving baryons would proceed at precisely the same rate as the C- or CP-conjugate processes involving antibaryons, with the overall effect that no baryon asymmetry is generated. Although C symmetry is maximally violated in the standard model, CP violation is only violated to a very small extent through the Kobayashi-Maskawa mechanism and is unable to account for the measured baryon asymmetry [14].
Like neutrinos, quarks also mix and this behaviour is described by their analog of the PMNS matrix called the Cabibbo-Kobayashi-Maskawa matrix or CKM for short. Both of these matrices contain complex phases that are called the CP violating phase. These phases, you guessed it, quantify the CP violating behaviour of interactions involving these particles. The CKM matrix looks just like the PMNS matrix and in the standard parametrization looks like:

$$\begin{bmatrix} V_{ud} & V_{us} & V_{ub} \\ V_{cd} & V_{cs} & V_{cb} \\ V_{td} & V_{ts} & V_{tb} \end{bmatrix} = \begin{bmatrix} 1 & 0 & 0 \\ 0 & c_{23} & s_{23} \\ 0 & -s_{23} & c_{23} \end{bmatrix} \begin{bmatrix} c_{13} & 0 & s_{13}e^{i\delta_{13}} \\ 0 & 1 & 0 \\ -s_{13}e^{i\delta_{13}} & 0 & c_{13} \end{bmatrix} \begin{bmatrix} c_{12} & s_{12} & 0 \\ -s_{12} & c_{12} & 0 \\ 0 & 0 & 1 \end{bmatrix}, \tag{1.37}$$

with δ_{13} the CP violating phase. The CKM can be written in many bases. But there is an invariant way of quantifying the CP violating behaviour through the so called Jarlskog invariant [15]:

$$J = c_{12}c_{23}c_{13}^2 s_{12}s_{23}s_{13}\sin\delta. \tag{1.38}$$

This invariant when appropriately normalised is roughly of the order 10^{-20} and is unfortunately too small to generate the η as measured.

3. **Out of equilibrium dynamics**. A dynamical process is said to be out of equilibrium if the expansion of the universe outpaces the reaction rate of the process. In order for baryon symmetry to occur this must also be the case for the process that generates it because in thermal equilibrium it is possible for pairs of antiparticles to annihilate each other. Departure from thermal equilibrium is therefore a necessary condition for the phenomenon of baryon asymmetry to occur since it freezes out the asymmetric particle configuration.
   An out of equilibrium state can be provided by the electroweak phase transition. A phenomenon that occurs shortly after the big bang where the Higgs potential acquires a non trivial vacuum expectation value. The way it can do this can be either through a first or second order phase transition. It has been determined that a second order phase transition cannot provide the desired departure from thermal equilibrium thus a first order phase transition is necessary[16]. You can see (see figure 1.1) that at the critical temperature there are two degenerate minima separated by a potential barrier. It is possible to tunnel through this barrier and small vacuum bubbles are created that expand and eventually take over all space. The non equilibrium condition is provided as the particles interact with the bubble wall as it sweeps through the plasma. The order of the electroweak phase transition depends on several factors including the mass of the Higgs boson. In order for a first order EWPT to occur, the Higgs mass must be contrained by an upper bound [17]. This is also the case for the supression of the sphaleron rate in the unbroken phase and these two considerations constrain the Higgs mass to $m_H < 35GeV$. Since the Higgs mass is $m_H \approx 1250GeV$, standard model physics is insufficient to satisfy also the last Sakharov condition.

1.3 Dark Matter

In 1933 Fritz Zwicky observed apparent anomalies in the velocity dispersion of the galaxies in the Coma cluster. The outer galaxies moved much faster than

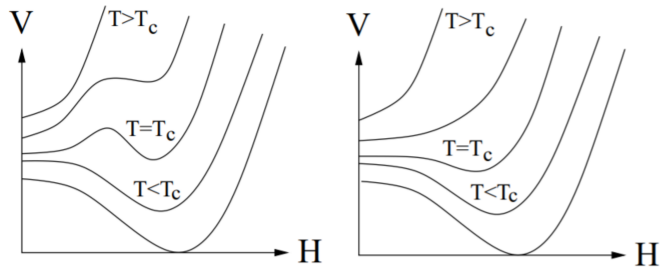

Figure 1.1: Schematic diagram of the difference between first and second order phase transition.

predictions made by considering all the observable matter present in that cluster. Similar behaviour was later observed in 1939 the Andromeda galaxy (M31) where the outer stars appeared to move way faster than predicted by the laws of gravity. See fig 1.2. Over time people began to postulate various explanations, the most convincing of which seemed to be dark matter: non-luminous matter that that can explain the deficit of observed mass that causes the movement of celestial bodies to deviate from what they were expected to be.
Observations of gravitational lensing is also a strong indicator of the presence of dark matter. Distortions in the images of background galaxies are used to probe the amount of mass needed to bring about such an observation. It turns out that often the lensing is stronger than naive assumptions predict. Dark matter is again in many cases a promising explanation for this phenomenon and assuming that dark matter indeed exists, gravitational (micro)lensing can be a good way of characterizing its distribution throughout the universe.
As experiments went on, it quickly became apparent that dark matter is omnipresent throughout our universe and even more so, is more abundant than luminous matter (roughly 85% of matter in our universe seems to be dark).
Postulating dark matter brings up the next question: What kind of matter? Dark matter can be divided into two categories, baryonic, and non-baryonic. Baryonic consists of most common objects known to astronomers such as stars, planets and black holes. Black holes, burnt-out dwarfs and other hard to detect dim bodies can in theory contribute to dark matter. Objects like this are called MACHOS (Massive Astrophysical Compact Halo Objects). However, the power spectrum of the cosmic microwave background (CMB) radiation temperature anisotropy proves that the baryon density in the universe is way smaller than of all the other gravitational matter. This, among other pieces of evidence suggest that baryonic dark matter cannot account for all dark matter present in the universe.
So, the extra matter has to be composed of something different from the ordinary particles. These are obviously particles that are not compositions of quarks but

are just single elementary particles. These particles must clearly be massive and interact extremely weakly, the only known particles that satisfy these criteria are neutrinos which unfortunately also are not heavy or abundant enough to make up all of the dark matter. Even if they were abundant enough, the Tremaine-Gunn bound places a lower limit on the a neutrino mass due to the limited volume fermions can occupy in phase space which exceeds the current upper bound of the neutrino mass. Therefore not enough neutrinos can be packed into a galaxy to form a dark matter halo. And even if the neutrino was massive enough it would quickly smear out density fluctuations that would hinder small structure formation. These arguments exclude Standard Model particles from being responsible for all dark matter.
Therefore over the last few decades a slew of hypothetical particles yet to be detected or excluded from existence were conjectured. Some of these are, axions, supersymmetric particles or WIMPs (Weakly Interacting Massive Particles). The non baryonic dark matter is often divided in hot dark mater (HDM), cold dark matter (CDM) or warm dark matter (WDM) depending on the velocities of the particles at the time they decoupled. Hot dark matter however is mainly excluded as being a candidate for DM due to the fact that they smear out density fluctuations just like neutrinos as mentioned in the previous paragraph and can thus only create large structures. Similarly, because colder structures are easier to cluster gravitationally, WDM can allow for structures of moderate size and CDM for objects of any size.
Various observations of large-scale structures suggest that cold dark matter is predominantly responsible for dark matter. The only downside of this is that in the standard model there is no suitable candidate to fulfill this role (neither are there for HDM or WDM). Many of the hypothetical cold dark matter particles that have been proposed to solve this problem fall into the WIMP category, so does the heavy neutral lepton or sterile neutrino, which will be central in this thesis.

1.4 Portals

Several models of weakly interacting particles have been proposed that have the potential to be dark matter or serve as mediators between the standard model and hidden sectors outside of it. Such mediators are sometimes called portals. Portals are classified by the particles doing the mediation. We will list three of them below:

1. **Scalar portal.** The Lagrangian density of the scalar portal looks like:

$$\mathcal{L} = \alpha_1 H^\dagger H S + \alpha_2 H^\dagger H S^2, \tag{1.39}$$

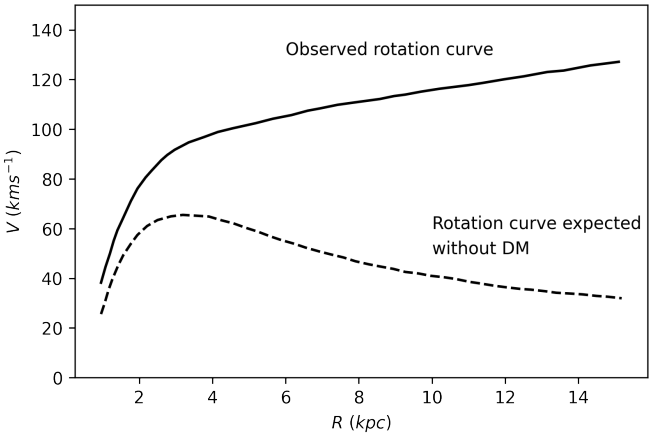

Figure 1.2: Rotation curves of M33 compared to naive expectation [18].

with H being the Higgs doublet and S a scalar and $\alpha_{1/2}$ real couplings. The particle behaves similar to the Higgs particle but its interaction is suppressed by a certain parameter $\theta \ll 1$ often called a mixing angle. The scalar S might be able to solve two problems; it might be responsible for inflation [19] or be a mediator for a hidden sector [20].

2. **Neutrino Portal.** As mentioned before the heavy neutral lepton is a promising candidate for dark matter, it also is potentially able to account for the other two BSM phenomena as well. It appears as an extension of the standard model as:

$$\mathcal{L} = F_{\alpha I}\overline{L}_{\alpha}\tilde{H}N_I + \text{majorana mass term} \tag{1.40}$$

Where L_α is the SM lepton doublet with $\alpha \in \{e, \mu, \tau\}$, $\tilde{H}$ the conjugated Higgs doublet and $F_{\alpha I}$ complex Yukawa couplings. N_I is the heavy neutral lepton (HNL) that interacts like the neutrino with the SM but just like the scalar portal it is suppressed by a mixing angle U_α.

3. **Vector portal.**

$$\mathcal{L} = \frac{\epsilon}{2}F_{\mu\nu}V^{\mu\nu} \tag{1.41}$$

Here $F_{\mu\nu}$ is the familiar gauge field associated with the $U(1)$ group of the standard model and $V^{\mu\nu}$ the field strength tensor of the so called dark photon.

1.5 Outline of this Thesis

We can conclude that while processes are possible within the physics of the standard model that can account for at least a small portion of the above mentioned

phenomena, they are by no means sufficient. Countless theories have been proposed to extend the standard model or even the laws of gravity to account for this. What we will focus on in this thesis is an extension of the standard model with new fields, who's excitations will be called the heavy neutral leptons or HNLs for short. These particles potentially have the ability to solve all three beyond standard model (BSM) phenomena at once. They are sterile, meaning non-interacting, heavy and may be able to explain the baryon asymmetry through leptogenesis. [21]. We will explain the relevant theory of HNLs, how they can explain the small but finite neutrino mass through the so called seesaw mechanism, how these particle might be produced in experiments and how their decay products can be detected. Then we will look at a host of experiments currently on their way and try to compare them as consistently as possible and we will compare these results with previous estimations from the literature.

Chapter 2

Heavy Neutral Leptons

To explain dark matter, it is an obvious choice to postulate a particle that is massive and extremely weakly interacting. The only known particle that satisfies this is the neutrino but as outlined in the previous section, they are unable to explain all the dark matter indirectly observed in the universe. In the previous section we stated that no right handed neutrinos are not observed, but the fact that right handed neutrinos are not observed of course does not guaranty that they do not exist. In fact, posing the existence of a right handed neutrino with a Majorana mass as a $SU(2)$ gauge singlet which therefore does not take part in the weak interaction seems to be a simple but powerful extension of the SM that can explain a host of phenomena.
Not only do the three phenomena introduced in the previous section hint at this new physics. Many anomalies in experimental particle physics such as the LSND anomaly [22] where an excess of electron antineutrinos were found in an muon antineutrino beam was found can be potentially attributed.
In light of the various non trivialities surrounding the neutrino mass outlined in section 1.1.1, it leaves us no choice but to extend the standard model. One of the simplest ways of doing this is by postulating the existence of gauge singlet Majorana fermions also called sterile neutrinos, right-handed neutrinos or heavy neutral leptons (HNLs). HNLs in the MeV-GeV range can explain the baryon asymmetry of the universe and at least two of them are needed to do so while a third HNL in the KeV range might be able to explain dark matter [23].

2.1 The Seesaw Mechanism

The neutrino might have mass, but its size is very small relative to other elementary particles ($\sum m_\nu < 0.12eV$ [6]). It is another hint at potential new physics and also the HNL can aid in elucidating the smallness of the neutrino mass. Let us look at the most common Lagrangian involving HNLs:

$$\mathcal{L} = \mathcal{L}_{SM} + i\overline{\nu_{Ri}}\partial\!\!\!/\nu_{Ri} + F_{\alpha i}\bar{L}_\alpha\tilde{H}\nu_{Ri} - \frac{1}{2}M^M_{ij}\overline{\nu^c_{Ri}}\nu_{Rj} + h.c., \tag{2.1}$$

with $F_{\alpha i}$ the Yukawa couplings, $\tilde{H}$ the conjugated Higgs doublet and $L_\alpha = (l_\alpha, \nu_{L\alpha})$ the lepton doublet where α runs over all lepton flavours and i over all right handed neutrinos. In this section we choose 3 right handed neutrinos for symmetry but the formalism can be altered to include an arbitrary number of them. Note that the third term is akin to eq. 1.23 and the fourth a Majorana mass term that is warranted by the fact that the ν_{Ri} are gauge singlets. So again after spontaneous symmetry breaking we arrive at a Dirac mass for this term:

$$M^D_{\alpha i} = \frac{F_{\alpha i}v}{\sqrt{2}}. \tag{2.2}$$

The Lagrangian of our theory then becomes:

$$\mathcal{L} = \mathcal{L}_{SM} + i\overline{\nu_{Ri}}\partial\!\!\!/\nu_{Ri} + M^D_{\alpha i}\bar{\nu}_{L\alpha}\nu_{Ri} - \frac{1}{2}M^M_{ij}\overline{\nu^c_{Ri}}\nu_{Rj} + h.c. \tag{2.3}$$

Upon closer inspection we can put the massive part of the Lagrangian in a matrix form:

$$\mathcal{L}_{\text{HNL mass}} = -\frac{1}{2}\begin{bmatrix}\overline{\nu_L} & \overline{\nu^c_R}\end{bmatrix}\begin{bmatrix}0 & M^D\\ (M^D)^T & M^M\end{bmatrix}\begin{bmatrix}\nu^c_L\\ \nu_R\end{bmatrix} + h.c. \tag{2.4}$$

Where we have ignored the indices. We can block diagonalize the mass matrix in the middle with the aid of an anti hermitian matrix W:

$$\mathcal{M} = W^\dagger\begin{bmatrix}0 & M^D\\ (M^D)^T & M^M\end{bmatrix}W^* = \begin{bmatrix}m_\nu & 0\\ 0 & M_N\end{bmatrix}. \tag{2.5}$$

Where W has the form

$$W = \exp\left(\begin{bmatrix}0 & \theta\\ -\theta^\dagger & 0\end{bmatrix}\right). \tag{2.6}$$

Which for small enough θ can be approximated to second order by

$$W \simeq \begin{bmatrix}1 - \frac{1}{2}\theta\theta^\dagger & \theta\\ -\theta^\dagger & 1 - \frac{1}{2}\theta^\dagger\theta\end{bmatrix}. \tag{2.7}$$

Version of August 9, 2023– Created August 9, 2023 - 19:58

From this it follows that

$$\theta \simeq M^D (M^M)^{-1} \tag{2.8}$$

And the mass matrices can be approximated as:

$$m_\nu \simeq -M^D \theta^T \simeq -M^D (M^M)^{-1} (M^D)^T = -\theta M^M \theta^T, \qquad M_N \simeq M^M \tag{2.9}$$

This is the well known seesaw formula [24–29] where the term seesaw comes from the fact that the light neutrino mass becomes smaller as the Majorana mass becomes bigger:

$$\begin{bmatrix} \nu_L^c \\ \nu_R \end{bmatrix} \xrightarrow{\text{mass basis}} \begin{bmatrix} \nu_{\text{light}} \\ N_{\text{heavy}} \end{bmatrix} \tag{2.10}$$

This mechanism could explain the smallness of the neutrino mass discussed earlier. For more information see [30]. We can see that in the mass basis the heavy states with mass M which we usually denote as N and call *heavy neutral leptons* (HNLs) are a mix of the right and left handed neutrinos and can hence interact with other particles. Only their interaction is suppressed by the so called mixing angles in θ. And of course therefore, SM neutrinos are a mix of their light mass eigenstates like we saw before in the section on neutrino oscillations plus a mix of the new heavy eigenstates:

$$\nu_{L\alpha} = V^{\text{PMNS}}_{\alpha i} \nu_i + \theta_{\alpha I} N_I^c \tag{2.11}$$

Where V^{PMNS} is the familiar PMNS mixing matrix. The absolute value squared of the mixing angles quantifies how suppressed the HNLs are in comparison to their light counterparts. It is therefore common to define the following quantities [31]:

$$U^2_{\alpha I} \equiv |\theta_{\alpha I}|^2, \qquad U^2_I = \sum_\alpha U^2_{\alpha I}, \qquad U^2_\alpha = \sum_I U^2_{\alpha I} \tag{2.12}$$

Otherwise, the HNLs interact in the same way with the SM model fields in the same way [32]:

$$\mathcal{L}_{int} = \frac{g}{2\sqrt{2}} W^+_\mu \overline{\nu^c} \sum_\alpha \theta^*_\alpha \gamma^\mu (1-\gamma_5) l^-_\alpha + \frac{g}{4\cos\theta_W} Z_\mu \overline{\nu^c} \sum_\alpha \theta^*_\alpha \gamma^\mu (1-\gamma_5) \nu^-_\alpha + h.c. \tag{2.13}$$

There are also other types of seesaw mechanisms. The one discussed here is the type-I seesaw mechanism characterized by the SM singlet. The other two are likewise characterized by the exchanged heavy particle. We will list these three below:

1. **Type I**: $SU(3) \times SU(2) \times U(1)$-singlet fermions
2. **Type II**: $SU(2)$-triplet scalars
3. **Type III**: $SU(2)$-triplet fermions

For more discussion see [21].

Version of August 9, 2023– Created August 9, 2023 - 19:58

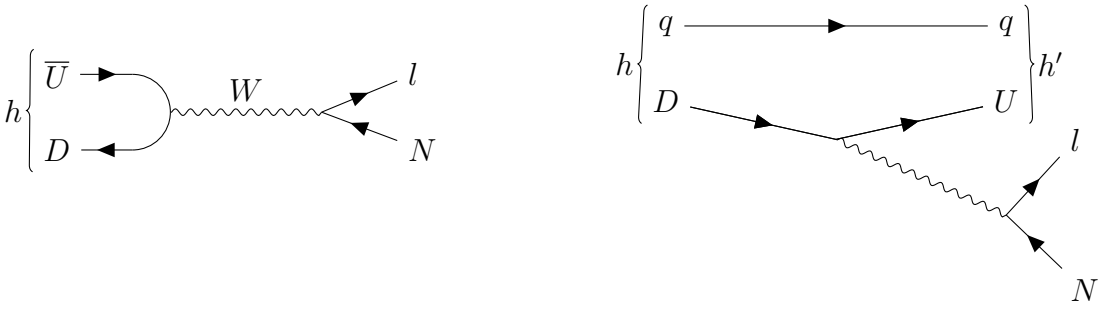

Figure 2.1: The leptonic (left) and semileptonic (right) decay of a hadron h. Here $D \in \{d, s, b\}$ and $U \in \{u, c, t\}$.

2.2 HNL Production

We will draw most of the relevant information in this section from the paper "*Phenomenology of GeV-scale heavy neutral leptons* [32]" by K. Bondarenko, A. Boyarsky, D. Gorbunov, and O. Ruchayskiy.

The production of heavy neutral leptons occurs mainly through the leptonic or semileptonic decay of mesons mediated by W bosons (see fig.2.1). The lightest of which (and therefore the most abundant) would be the main sources of HNLs if they exist. Such particles are π mesons ~ 0.14 GeV or kaons (K meson) ~ 0.5 GeV. However, experiments have already excluded a significant portion of the parameter space below the kaon mass [33]. In this thesis we will therefore mainly focus on HNL masses > 0.5 GeV.
Mesons with such masses which are most relevant for HNL production are the charmed D mesons with masses ~ 2 GeV: $D^0(c\overline{u}, 1865)$, $D^+(c\overline{d}, 1870)$, $D^+(d\overline{c}, 1870)$, and $D_s(c\overline{s}, 1968)$, and the beauty mesons $B^-(b\overline{u}, 5279)$, $B^0(b\overline{d}, 5280)$, $B_s(b\overline{s}, 5367)$ and $B_c(b\overline{c}, 6276)$ who have their masses in the range $\sim 5 - 6$ GeV.

Let us first look at the charmed D mesons. The D^0 meson is neutral so weak decay through a charged current yields a meson in the final state. This limits the mass of the HNL being produced from this decay quite a bit. Considering the largest branching ratio of such a process which is a decay to a K meson, the mass of the HNL is limited to be: $M_N < M_{D^0} - M_K \approx 1.4$ GeV. The charged mesons like the $D^\pm$ and the D_s meson may decay into two bodies like the left diagram in fig.2.1. And given the mass of the other lepton being much smaller the HNL produced in this process can be almost as heavy as the D meson itself. The meson with the highest branching ratio is the D_s meson which is about a factor 10 higher than others for decays of the form $D \to N + X$ (see fig. 2.3). And although D_s is harder to produce due to its heavier mass, its production is only suppressed by a

small factor [34]. This makes D_s the main source for HNLs in our experiments.

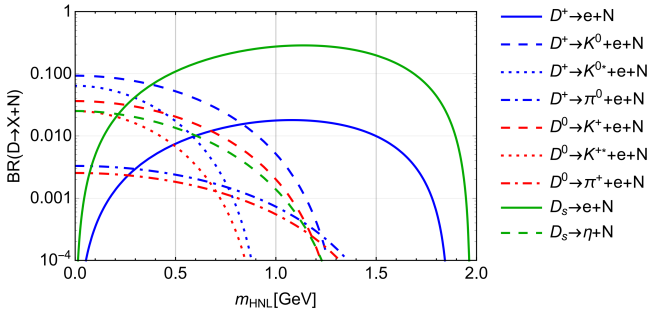

Figure 2.2: The dominant branching ratios for the production of HNLs from charmed mesons for $U_e = 1$, $U_\mu = U_\tau = 0$ [32].

Similarly to the D^0 meson the neutral B^0 and B_s beauty mesons also decay through the semileptonic decay with another meson in the final state. These will mostly decay to D mesons so the HNL mass is constrained to be $M_B - M_D \approx 3.4$ GeV. The charged beauty mesons $B^\pm$ and $B_c^\pm$ decay leptonically and again are able to produce HNLs that are roughly of the same mass. Due to CKM suppression the branching ratio for the process $B^+ \to N + l^+$ is suppressed compared to the branching ration of $B_c \to N + l$ but the production fraction is of order $\mathcal{O}(10^{-3})$ and is only measured ad LHC energies and is unknown for lower energies [35].

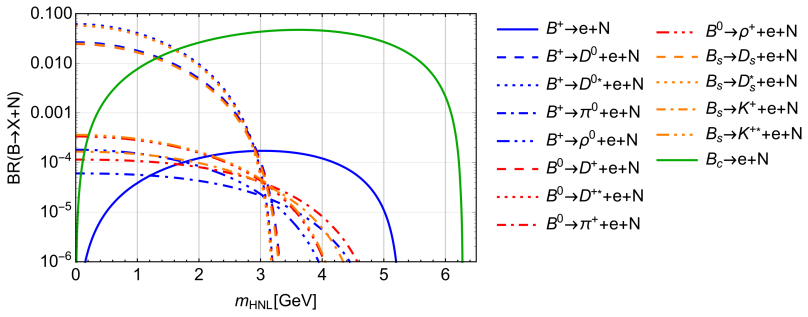

Figure 2.3: The dominant branching ratios for the production of HNLs from beauty mesons for $U_e = 1$, $U_\mu = U_\tau = 0$ [32].

2.3 HNL Decay

As can be seen from eq. 2.13, the HNL decay is mediated by charged or neutral weak currents. In figure 2.6 this is shown by two Feynman diagrams and these

Version of August 9, 2023– Created August 9, 2023 - 19:58

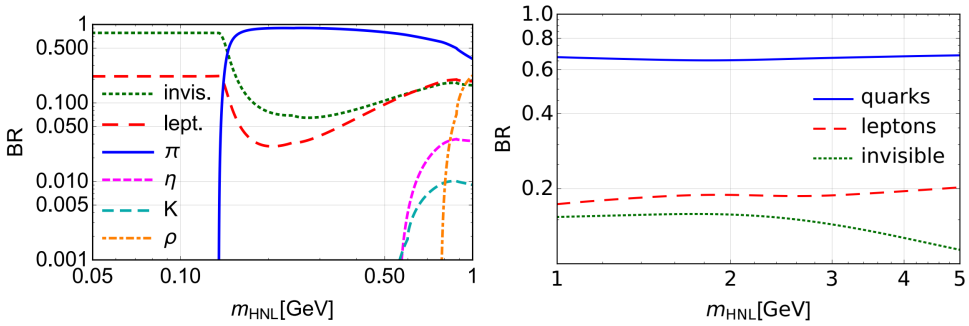

Figure 2.4: Branching ratios for various decay products of the HNL. For this figure the mixing ratio is $U_e : U_\mu : U_\tau = 1 : 1 : 1$ [32].

are involved in all HNL decay processes. In our model the HNLs are Majorana particles. This means that all the reactions discussed above can also happen in their charge conjugated form. This makes the possible decay paths twice as large as opposed to Dirac particles and therefore the decay width should also be enlarged by a factor of two.

For the charged decays (mediated by the W boson) the particles labelled U and D could be an up-down quark pair (u_i, d_j) or a lepton pair (ν_α, l_α) and the f in the neutral decay product can be any lepton. In the case of two quarks in the final state they can hadronize into a new meson.

The decay products can help to validate the HNLs existence or not, but not all potential decay modes will be detectable. Specifically the neutral current decay into three neutrinos:

$$N \to \nu_\alpha + \nu_\beta + \overline{\nu}_\beta$$

The reason for this is obvious; neutrinos are hard to detect.

For the mass region above the pion mass, semileptonic HNL decay becomes dominant. We can see from fig. 2.5 that above 2 GeV the ratio between the combined decay width into single-meson final states becomes less than decay into quarks. This means that in that in this range multi meson final states start to become significant. See fig. 2.7 for an example of an HNL decaying into two kaons and a lepton.

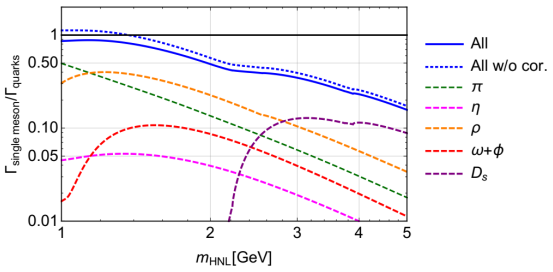

Figure 2.5: HNL decay widths into relevant single meson channels, divided by the total decay width into quarks. The solid blue line is the combined decay width of all mesons divided by the decay width of decay into quarks with QCD corrections the dotted blue line without QCD corrections. For more information see [32].

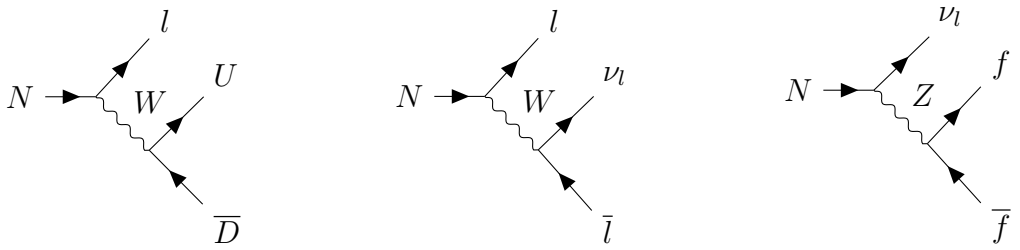

Figure 2.6: Different possible paths of HNL decay mediated by neutral or charged currents. Again $D \in \{d, s, b\}$ and $U \in \{u, c, t\}$.

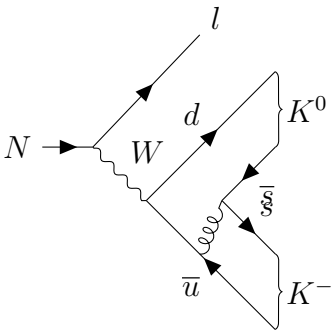

Figure 2.7: Example of a multimeson final state where an HNL decays into two kaons.

Chapter 3

Experimental Searches for HNLs

There have been many efforts to look for heavy neutral leptons and many more are on the way. Experiments range from collider searches to cosmological and astrophysical searches (see [36] for an overview). The first experiments looking for HNLs started in the mid 1980s where the experiments PS191 [37] placed the first bounds on the mass-mixing parameter space. In this thesis we will focus mainly on collider searches that are mainly based at CERN. We will lay out their specifics in the following sections.

3.1 Extracted Beam Lines at CERN

Extracted beam line experiments as the name states, are experiments that extract a portion of a beam from a cyclotron and then dump it into a target (these experiments are also called beam dump experiments). Historically extracted beam line experiments were the first to look for HNLs like the previously mentioned PS191 experiments and the CHARM [38] and NOMAD [39] experiments. Some of the heaviest constraints on the HNL decay are obtained by recent experiments at PIENU [40], NA62 [41], T2K [42], MicroBooNE [43], and ArgoNeuT [44].
Since HNLs interact weakly many particle interactions must be needed in order to conclusively witness a rare event. That is why experiments looking for hidden particles use high intensity beams and are denoted as *intensity frontier* experiment as opposed to *energy frontier* experiments such as the LHC that can reach energies in the neighbourhood of 13.6 TeV. It must be said however that the high luminosity of the LHC in run 3 and further also places it in the intensity frontier. In this section we will consider three promising experiments at CERN: SHiP, NA62 and SHADOWS. We will outline their way of operating and other relevant parameters.

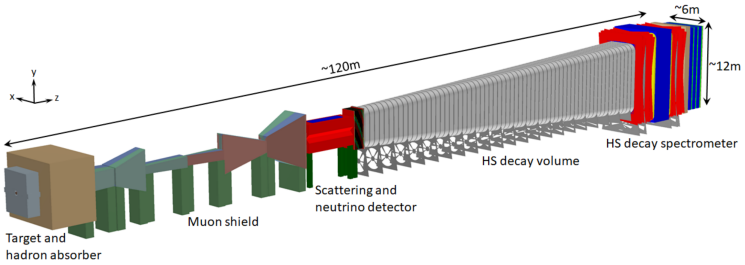

Figure 3.1: Outline of the SHiP experiment [45].

3.1.1 SHiP

The Search for Hidden Particles or SHiP [45] for short is an experiment to be located at the so called Beam Dump Facility (BDF) at CERN approximately 15 meters under ground. It's purpose is to probe various proposed new physics which involves particles with masses up to $\mathcal{O}(10GeV)$. It is fed by the SPS accelerator with a 400 GeV proton beam which delivers approximately 2×10^{20} POT over a 5 year period. The beam collides with a titanium-zirconium doped molybdenum alloy (TZM) followed by blocks of tungsten [45]. The beam is then passed through a 5 meter hadron stopper designed to get rid of $\pi^{\pm}$ particles and K mesons. Then comes a 34 meter muon shield consisting of magnets to deflect muons from entering the decay volume to further mitigate background. The decay volume starts approximately 50 meters from the target and is a 50 meter long pyramidal frustum vacuum chamber. The detector on the end of the decay volume is a spectrometer consisting of a four-station tracker, timing detector, an electromagnetic calorimeter and muon detector which helps particle identification.

3.1.2 NA62

The NA62 experiment originally was designed to study the rare decays of kaons [46]. It too uses a 400 GeV proton beam from the SPS called the P42/K12 beamline that strikes a a 400 mm long beryllium target that produces a collimated beam of charged pions (π^+), kaons (K^+) and protons (p) with a momentum of around 75 GeV. The decay volume is about 80 meters in length and sits at a distance of about 100 meters from the target. The first run collected data generated from about 2.2×10^{18} POT K^+ particles produces a neutrino when decaying which can hypothetically mix with an HNL with a mass up to about 0.45 GeV. In the past the NA62 experiment has already placed upper bounds on the HNL with data of its first run by studying the decays $K^+ \to e^+ + N$ and $K^+ \to \mu^+ + N$ [47].
A proposal has been made to slightly alter the setup of the NA62 experiment by removing the Beryllium target and thereby letting the beam directly hit a pair of

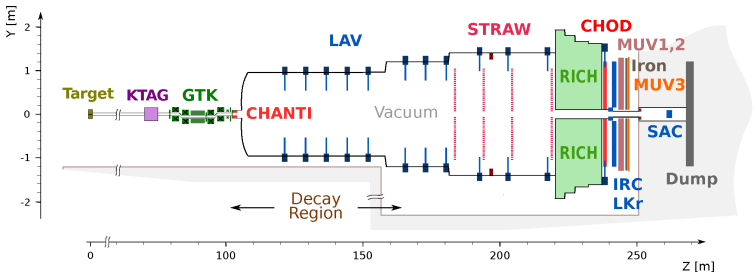

Figure 3.2: Layout of the NA62 experiment [48].

Cu-Fe collimators that are placed between bending dipole magnets. This setup is called dump mode as whereas the normal setup is called beam mode. The dump mode will allow for the production of particles like charmed hadrons and therefore will allow to probe a larger region of parameter space for HNLs. It is expected that this experiment will eventually gather around 5×10^{19} POT between 2032 and 2038.

3.1.3 SHADOWS

The SHADOWS (Search for Hidden And Dark Objects With the SPS) [49] experiment uses the same P42/K12 beamline as the NA62 experiment and will also be built in the same location (hall ECN3). The detector will be placed off axis with respect to the beam since charm and beauty mesons can have a significant amount of transverse momentum. The detector is placed 10 meter from the target, is roughly 20 meters in length and its transverse dimensions are 2.5×2.5 meters. The fact that the detector is off-axis makes it easier for the detector to be close to the interaction point. This has the advantage of reducing background since this is mostly concentrated in the forward direction and also allows for a better geometrical acceptance. It is expected to take data from about 5×10^{19} POT from separate runs which are estimated to be finished between 2032 and 2038.

3.2 LHC based Experiments

The LHC is the worlds largest and most powerful collider. It scatters protons onto protons with a record center of mass energy of $\sqrt{s} = 13.6$ TeV. It has four interaction points with a total of nine experiments divided among those. The LHC had a central role in testing the standard model but presently has plenty of programs that are trying to probe physics outside of the SM. In this section we will look at some of such promising programs proposed that are specifically designed to search for long lived feebly interacting particles (FIPs) at the LHC.

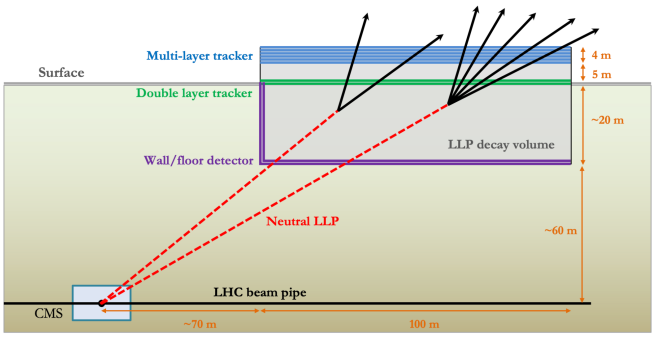

Figure 3.3: Side view of the MATHUSLA setup [50].

3.2.1 MATHUSLA

MATHUSLA (MAssive Timing Hodoscope for Ultra Stable neutraL pArticles) is a detector proposed to be built on the surface above either the ATLAS or CMS detector. It will cover an area of 200×200 meters and will have a height of about 20 meters. The detector makes use of of passive shielding provided by $\sim$ 100 meters of rock between the collision point and the experiment. Any sufficiently long lived particle that might decay in the decay volume of the detector is then aimed to be detected by particle detectors in the roof of the construction. See fig. 3.3 for a drawing of the setup.

3.2.2 Codex-b

Codex-b is a detector closer to the collision point. It also is designed to look for new physics particles. It is a $10 \times 10 \times 10$ m^3 cube shaped detector about 26 meters away from the LHCb experiment. It is shielded by a lead shield as a means to halt any hadronic particles coming from the interaction point. See figure 3.4 for the setup.

3.2.3 FASER

FASER (ForwArd Search ExpeRiment [52]) as the name implies is situated $\sim$ 480 meters away from the very forward region of the ATLAS detector in an service tunnel (TI12). It too makes use of passive shielding by rock $\sim$ 100 m and the large magnets of the LHC divert away a lot of charged background particles as well. The detector has a small angular acceptance due to its small size and measures about $|\theta| < 0.21$ mrad which corresponds to a pseudorapidity $\eta > 9.2$. The length of the detector is also relatively small at about 1.5 meters in length.
A second larger version of this experiment FASER2 is also proposed and will extend

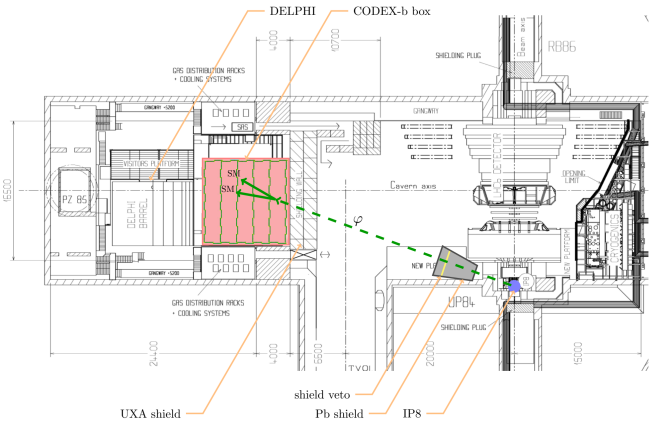

Figure 3.4: Top view of the Codex-b setup [51].

its sensitivity reach significantly over FASER. FASER2 will have a detector length of 5 meters and will have a magnetic aperture with a diameter of 2 meters ($\eta \gtrsim 6.9$) improving the acceptance from D and B meson decays.

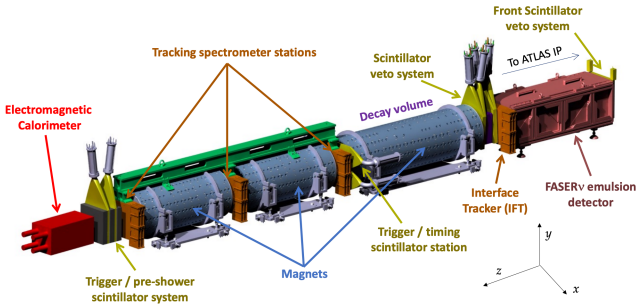

Figure 3.5: Top view of the Codex-b setup [52].

3.2.4 FACET

FACET (Forward Aperture CMS ExTension [53]) is an extension in the forward region of the CMS experiment designed to look for long-lived BSM phenomena among which are heavy neutral leptons. The detector will be ~ 100 meters away from the collision point and will be about 26 meters in length and will cover an angular size of about $7.6 > \eta > 6.2$. The detector will have a decay volume of about 18 meters followed by 8 meters of various detection equipment.

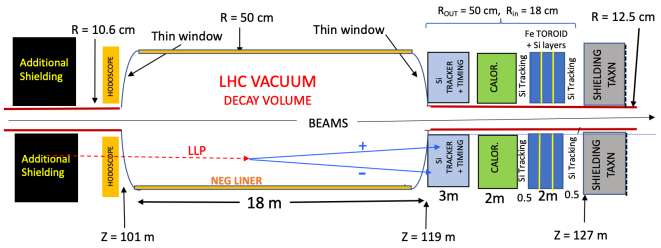

Figure 3.6: Schematic impression of the FACET detector. [54].

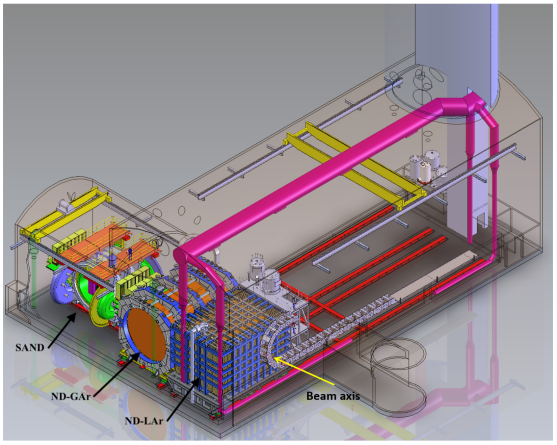

Figure 3.7: Computer model of a concept for the DUNE ND detector facility [55].

3.3 DUNE ND

The DUNE (Deep Underground Neutrino Experiment) [55] is a project currently on the way in Fermilab, Illinois to primarily study neutrinos. In particular it aims to measure the CP violating phase δ_{CP}, θ_{23} and the mass ordering of neutrinos. The experiment will have two detector a near detector (ND) at Fermilab and a far detector (FD) roughly 1300 km away in the Sanford Underground Research Facility. The neutrinos studied in the experiment are produced by a beam of 120 GeV protons delivering 1.1×10^{21} POT per year provided by the main injector accelerator. The beamline is named the "Long Baseline Neutrino Facility" (LBNF) where baseline refers to the distance between the collision point ant the detector. The proton beam is scattered on a graphite target and produced kaons and pions are focused by a so called magnetic horn into a decay volume where they decay into neutrinos. The weakly interacting neutrinos then reach the first detector (ND) and then travel 1300 km through earth to reach the detectors (FD) of the facility in Sanford.

The ND will be placed 574 m from the target and one of its main task will be to monitor the neutrino beam going to the FD. The design of the ND is not finalized but it will most probably will have a Liquid Argon Time Projection Chamber (LArTPC) caled the ND-LAr followed by a multipurpose detector consisting of a high pressure gaseous argon TPC and electromagnetic calorimeters. The final detector will be the SAND (System for on-Axis Neutrino Detection) and is used to monitor the flux of neutrinos going to the FD. See fig. 3.7 for an impression. Aside from monitoring the neutrino flux the DUNE ND can also search for potential new physics particles like the HNLs of the order of the D meson mass which is what we will be focusing on in this report.

Chapter 4

Sensitivities of Experiments

We will draw most of the relevant information in this section from the paper "*Sensitivity of the intensity frontier experiments for neutrino and scalar portals: analytic estimates*" by Bondarenko et al. [56]

Given a particular model, in our case the model for the HNL, one can begin to calculate cross sections and decay rates and infer from those results at what rate these particles can be created and how they decay as was discussed in chapter 2. Then, given the relevant parameters of a particular experiment, one can calculate how often an HNL production and decay can occur within the confines of the experiment.
There are of course unknowns in our model, like the mixing parameters U_α^2 (with $\alpha \in \{e, \mu, \tau\}$) and the mass of the HNL. These parameters are not constrained by the neutrino masses m_ν, it is only their combination as appearing in eq. (2.9) that is constrained. For example, naively $\theta^2 \sim \theta^2_{seesaw} = m_\nu/M_N$. But noting that the mixing matrix θ is complex and we for example choose 2 HNLs, a cancellation can happen, such that $M_N\theta_1^2 - M_N\theta_2^2 \sim m_\nu$ and at the same time $\theta^2 \ll m_\nu/M$. The fact that this is possible at all is an important remark, because we mainly explore exactly this region So we end up with a certain four dimensional parameter space consisting of U_α^2 and M_{HNL} four which we can check which region of this parameter space is able to be probed by our experiment. Usually we focus only on one mixing flavour at a time which commonly is U_e^2 which simplifies the analysis and makes it easy to graph visually.
In this thesis we employ relatively simple but robust techniques for estimating the sensitivities of experiments that allow for easy adjustment in the case of changes in the designs or estimates of production and decay of HNLs that often deals with physics that is outside of perturbative QCD and low-energy meson physics. The flexibility of this approach can be favourable over conventional and generally

superior Monte Carlo (MC) simulations which often have a limited amount of parameters and take more effort in order to adjust them.

4.1 How to Calculate the Sensitivity of an Experiment

Let us look at how to go about these sensitivity calculations. When the proton beam hits the target, a slew of particles is born a part of which fly in the direction of the detector. After all the background is hopefully mostly filtered out, the relevant particles, in our case the HNLs are left. Now we must know how many of mesons decay into an HNL for a given value of a mixing angle. Given that N_M mesons of certain type are created the fraction of M mesons that decay into HNLs is giving by the branching ratio $BR_{M\to X}$, where X denotes the HNL. So the number of relevant particles created is:

$$N_{\text{produced},M_i} = N_{M_i} \times BR_{M_i\to X}. \tag{4.1}$$

$M \in \{B, D\}$ denotes the type of meson and i and denotes which type of B or D meson. For D mesons we have $D_i \in \{D^+, D^0, D_s^+\}$ and for B mesons we have $B_i \in \{B^+, B^0, B_s, B_c^+\}$. $BR_{M_i\to X}$ is proportional to U_α^2 and since in this model this parameter is of course still unconstrained the number of particles depends on it. See fig. (4.3) where $BR_{M_i\to X}$ is plotted for $U_\alpha^2 = 1$. N_{M_i} is given by the total amount of B or D mesons multiplied by their fragmentation fraction f_{M_i}. Thus $N_{M_i} = f_{M_i} \times N_M$. The number of D or B mesons is in turn given by a factor that expresses the total amount of c or d quarks per POT ($N_{\mathbf{POT}}$) which we will call χ_q with $q \in \{c, d\}$. So the final expression yields:

$$N_{\text{produced},M_i} = N_{\text{POT}} \times \chi_q \times f_{M_i} \times BR_{M_i\to X}. \tag{4.2}$$

The mesons created from the proton beam have different momenta which dictates whether they fly in the direction of the beam and if they are likely to decay in the detector or not. The distribution of mesons with a certain absolute value momentum p and angle relative to the beam axis θ is enough to characterize the relevant properties of the particles of interest in our experiments since we assume that because of the cylindrical symmetry of our experiments the distribution is not dependant on the azimuthal angle ϕ. And we often denote the normalized distribution function as:

$$f_M(p, \theta) = \frac{1}{N_M}\frac{d^2N_M}{dpd\theta}. \tag{4.3}$$

Version of August 9, 2023– Created August 9, 2023 - 19:58

Often the distribution is given in terms of the pseudorapidity (η) and the transverse momentum P_T but the idea remains the same. We can infer the momentum of our HNL X from the momentum of the meson with some simple relativistic kinematics. Now we must calculate how likely it is for particle X with a certain momentum to decay inside the detector, the probability is given by:

$$P_{\text{dec},M} = e^{-\frac{l_{\text{target-det}}}{l_{\text{dec}}}} - e^{-\frac{l_{\text{target-det}}+l_{\text{det}}}{l_{\text{dec}}}}. \tag{4.4}$$

Where $l_{\text{target-det}}$ is the distance between the target and the decay volume of the detector, l_{det} is the length of the detector and l_{dec} is the decay length of the particle defined as:

$$l_{\text{dec}} = c\tau_X \beta_X \gamma_X, \tag{4.5}$$

with τ the lifetime of the particle β its velocity and γ the gamma factor. τ just like $BR_{M_i \to X}$ depends on the mixing angle but this time as: $\tau \propto U_{\prime\alpha}^{-2}$ (see fig 4.1). We estimate the gamma factor of the HNL from the gamma factor of the meson as:

$$\gamma_X \approx \gamma_{\text{meson}} \frac{E_X^{\text{rest}}}{M_X}, \tag{4.6}$$

where E_X^{rest} is the energy of the HNL in the rest frame of the meson which we approximate by looking at the expression for the energy of a particle in two body decay:

$$E_X^{\text{rest}} = \frac{M_M^2 + M_X^2 - m^2}{2M_M} \approx \frac{M_M}{2} + \frac{M_X^2}{2M_M} = \frac{M_M^2 + M_X^2}{2M_M}, \tag{4.7}$$

where we have made the approximation under the assumption that $m \ll M_X$ where m is the other product in the decay. Now using $\gamma_M = E_M/M_M$, we can express γ_X as follows

$$\gamma_X \approx \gamma_{\text{meson}} \frac{E_X^{\text{rest}}}{M_X} \approx \frac{E_M}{M_M M_X} \frac{M_M^2 + M_X^2}{2M_M} = E_M \frac{M_M^2 + M_X^2}{2M_M^2 M_X}. \tag{4.8}$$

We have now an expression for the detector length given the lifetime of the HNL as obtained from [32] (see fig. 4.1)

Now we have the expression for the probability of decay within the detector. Now we integrate it over the distribution function with appropriate boundaries for θ in accordance with the geometrical acceptance of the detector:

$$\int_0^\infty \int_{\theta_{min}}^{\theta_{max}} f_M(p,\theta) P_{\text{dec},M}(p, U_\alpha^2) d\theta dp$$

Where we have assumed the distribution function to be normalized. To account for the range of azimuthal angle that the detector covers we multiply this expression

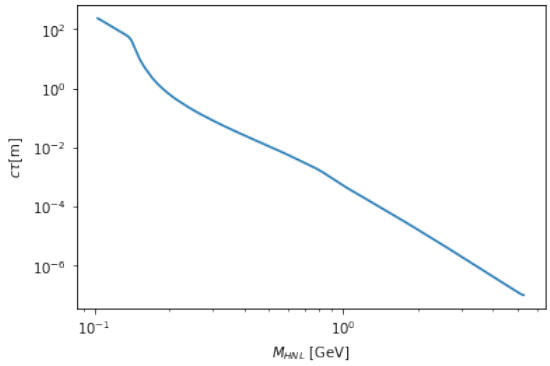

Figure 4.1: Proper lifetime of the HNL with electron mixing as a function of the HNL mass for $U_\alpha^2 = 1$. Data obtained from [32].

with a factor $\Delta\phi/2\pi$. With $\Delta\phi = \phi_{max} - \phi_{min}$. So now the number of HNLs decaying in our detector for a certain meson flavour is given by:

$$N_{M_i} \times BR_{M_i \to X} \times \frac{\Delta\phi}{2\pi} \times \int_0^\infty \int_{\theta_{min}}^{\theta_{max}} f_M(p,\theta) P_{\mathrm{dec},M}(p, U_\alpha^2) d\theta dp \tag{4.9}$$

However not all decay modes are detectable (for example when an HNL decay into three neutrinos), so we must multiply by the visible branching ratio (see fig. 4.2) which is the fraction of decays that are actually visible to the detector. The final thing we should take into account is the efficiency of the detector itself for various technical reasons a particle might not be detected even if it it decays inside the volume of the detector. This efficiency is done by studying simulations and the detector itself and the efficiency is given by the factor ϵ_{det}. So the total number of detected events in case our model is correct is predicted to be:

$$N_{\mathrm{events},M_i} = N_{\mathrm{produced},M_i} \times Br_{vis} \times \epsilon_{\mathrm{det}} \tag{4.10}$$

$$\times \frac{\Delta\phi}{2\pi} \int_0^\infty \int_{\theta_{min}}^{\theta_{max}} f_M(p,\theta) P_{\mathrm{dec},M}(p, U_\alpha^2) d\theta dp \tag{4.11}$$

So in the total amount of events is

$$N_{\mathrm{events}}(\theta_X, M_X) = \sum_{i,M} N_{\mathrm{events},M_i}(\theta_X, M_X) \tag{4.12}$$

Now the question is: how many events do we have to detect in order to conclude we have detected an HNL? The main factor that comes into play that determines the amount of signals needed for conclusive detection is the amount of

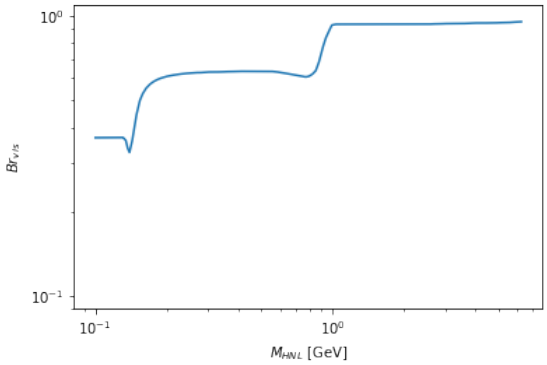

Figure 4.2: The visible branching ratio for HNL decay for electron mixing only. Data obtained from [32].

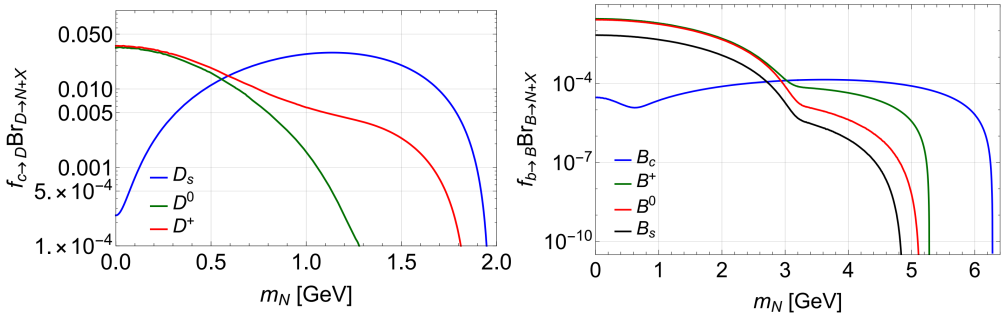

Figure 4.3: The branching ratios for D and B mesons for electron mixing only. Data obtained from [32].

background particles which fortunately are very low for our experiments see for example the background considerations of SHiP ([57], [58], [59], [60]) and MATHUSLA ([61],[62]). Although even with background $N_{\text{background}} \ll 1$ the amount of particle that need to be detected is still around 2.3 for 90% certainty [56]. So to get the total sensitivity reach we require:

$$N_{\text{events}}(\theta_X, M_X) \geq 2.3 \tag{4.13}$$

We display this using a contour plot.

4.2 Upper and Lower Boundaries of Sensitivity Curves

If an HNL is extremely weakly interacting (small U_α) it might not decay until it has passed the detector volume in that case

$$l_{\text{dec}} \gg l_{\text{det}}, l_{\text{target, det}}.$$

We can therefore approximate eq. (4.4) as:

$$P_{\text{dec},M} \approx \frac{l_{\text{det}}}{\text{dec}} = \frac{l_{\text{det}}}{c\tau_X \langle \gamma_X \rangle} \tag{4.14}$$

Where we have assumed the particle to be relativistic and thus $\beta \approx 1$. In this approximation the number of events inside the detector is:

$$N_{\text{events lower}} \approx N_{\text{meson}} \times BR_{M\to X} \times \frac{l_{\text{det}}}{c\tau_X \langle \gamma_X \rangle} \propto U_\alpha^4 / \langle \gamma_X \rangle \tag{4.15}$$

This equation describes the lower bound of the sensitivity curve.

To estimate the upper boundary we look at the case where the coupling is sufficiently strong so that the HNL decays before it reaches the detector.

$$l_{\text{dec}} \ll l_{\text{det}}, l_{\text{target, det}}.$$

The maximum mass able to be probed by the experiment is where the upper and the lower boundaries meet (see figure 4.4).

4.3 Distribution Functions

The distribution functions for the mesons vary between experiment and also within the same experiment there are multiple distributions available and no general consensus exists which is the best one. We strife to be as consistent as possible so we

Version of August 9, 2023– Created August 9, 2023 - 19:58

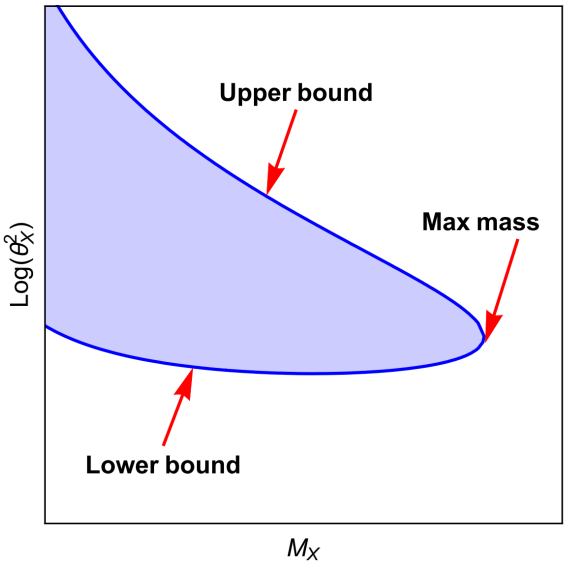

Figure 4.4: Schematic diagram of a typical sensitivity curve [56].

can at least make statements based on relative comparisons as opposed to absolute comparisons.

4.3.1 Distribution function of extracted beamline experiments

The distribution functions for the D and B mesons for the beam dump experiments SHiP, NA62 and SHADOWS is given in figure (4.5). The distribution has an odd shape due to most particle being created at small angles hence we have chosen to display it on a log-log for the θ and E axes. The awkward shape of the distribution also makes it difficult to smooth out the function by interpolation so we can properly integrate over it. That is why we integrate the distribution in log space which gives us an additional Jacobian factor in our integral:

$$\int_0^\infty \int_{\theta_{min}}^{\theta_{max}} \frac{d^2N_M}{dEd\theta} d\theta dE \longrightarrow \int_0^\infty \int_{\theta_{min}}^{\theta_{max}} \frac{d^2N_M}{d\log_{10}(E)d\log_{10}(\theta)} \frac{1}{\ln^2(10)\theta E} d\theta dE \tag{4.16}$$

4.3.2 Distribution of D and B mesons at the LHC

The distribution functions for D and B mesons at the LHC are given in figure 4.6. It is a function of the transverse momentum and the pseudorapidity defined as:

$$\eta = -\ln\left(\tan\frac{\theta}{2}\right) \tag{4.17}$$

Where θ is the angle of the particle's three momentum with the beam axis like usual.

4.3.3 Distribution of D mesons at DUNE

The energies at DUNE only allow for D meson production. The production can be described by:

$$\frac{dN}{dx_F dp_T^2} \propto \frac{d\sigma}{dx_F dp_T^2} \sim (1 - |x_F|)^n e^{-bp_T^2}, \tag{4.18}$$

where x_F is the so called Feynman-x defined as:

$$x_F = \frac{2p_z}{\sqrt{s}}. \tag{4.19}$$

Here p_z is the longitudinal momentum of the particle and $\sqrt{s}$ the invariant mass. Both the longitudinal momentum and the transverse momentum are evaluated in the center of mass (CM) frame of the proton nucleon reacting of the collider at DUNE. The values for n and d are determined by the so called E769 experiment and are fitted to be: $n = 6.1$ and $b = 1,08 GeV^{-2}$ [63]. See fig. (4.7) for a plot of the function in eq. 4.18.
To determine the geometrical acceptance we need to know the angle and absolute value momentum of the particle in the lab frame. We will do this be determining the value of the center of mass velocity and boosting along the longitudinal direction. The Lorentz transformation to the lab frame for momentum is

$$p_{z,\text{lab}} = \gamma(p_{z,\text{CM}} - v_{cm} E_{\text{CM}}). \tag{4.20}$$

The value of the center of mass velocity for particles with equal mass (assuming proton-proton collision) is given by:

$$v_{cm} = \frac{\sqrt{E_{lab} - m_p}}{\sqrt{E_{lab} + m_p}}, \tag{4.21}$$

with $E_{lab} = 120$ GeV. Which corresponds to a gamma factor of

$$\gamma \approx 8.0. \tag{4.22}$$

To calculate $p_z \equiv p_{z,\mathrm{CM}}$ we use relation 4.19:

$$p_z = x_F \frac{\sqrt{s}}{2}. \tag{4.23}$$

The invariant mass is the given by:

$$\sqrt{s} = \sqrt{(p_p^\mu + p_A^\mu)^2} = \sqrt{2m_p^2 + 2m_p E_{lab}} \approx 15.1 \text{ GeV}, \tag{4.24}$$

with p_A^μ the momentum of the nucleon. To calculate the E_{CM} we use the common relation $E_{CM} = \sqrt{p^2 + m_D^2} = \sqrt{p_z^2 + p_T^2 + m_D^2}$. Filling this into eq. (4.20) gives us our final expression:

$$p_{z,\mathrm{lab}} = \gamma \left(x_F \frac{\sqrt{s}}{2} + v_{cm} \sqrt{p_z^2 + p_T^2 + m_D^2} \right). \tag{4.25}$$

Where the plus sign is chosen so that the boost is in the proper direction. Now we can calculate the momentum and angle of the meson as desired:

$$p_{lab} = \sqrt{(p_{z,\mathrm{lab}}^2 + p_T^2)}, \qquad \theta_{lab} = \arctan\left(p_T / p_{z,\mathrm{lab}}\right) \tag{4.26}$$

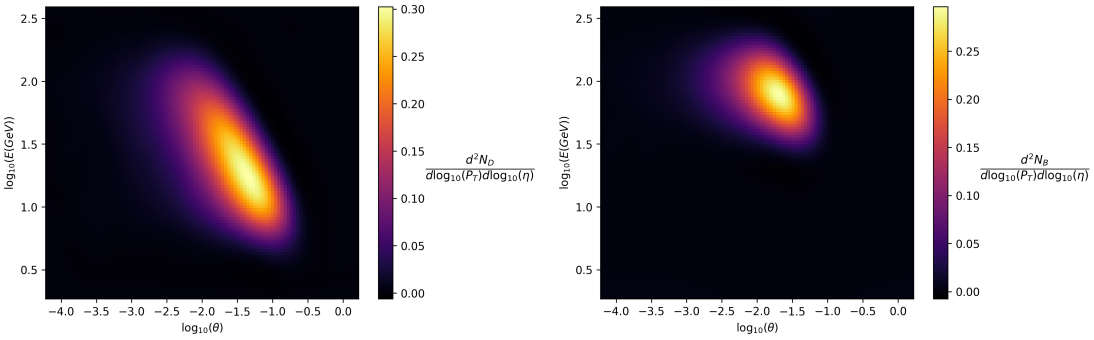

(a) D meson distribution (b) B meson distribution

Figure 4.5: Distribition for D and B meson production at the beam dump experiments fed by the 400 GeV beam of the SPS.

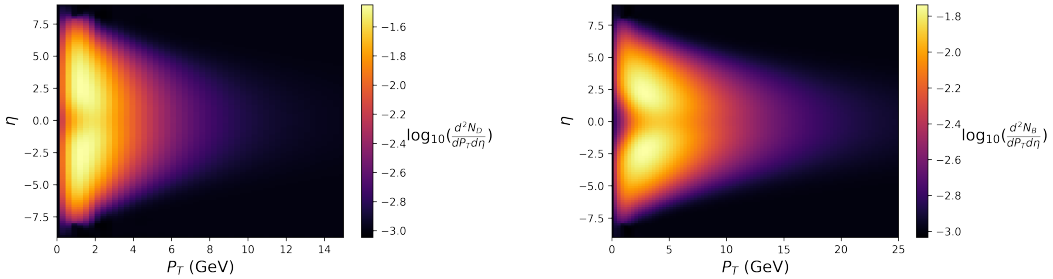

(a) D meson distribution (b) B meson distribution

Figure 4.6: Distribition for D and B meson production at the LHC.

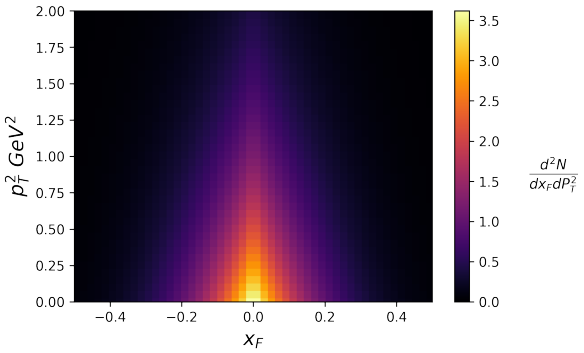

Figure 4.7: Distribution for D mesons at DUNE.

Version of August 9, 2023– Created August 9, 2023 - 19:58

Chapter 5

Results

We have finally all the information and tools needed to make a solid estimate of the sensitivities of the various intensity frontier experiments currently running or on the way mentioned earlier. In the following section we will show the results from plugging the relevant parameters into eq. (4.13) and plotting the contour in the (U_e^2, M_X) parameter space.

5.1 Results for Beam Dump Experiments at CERN

The relevant parameters for the experiments based on extracted beam lines at CERN are given in table 5.1. For D mesons we have $\chi_D = 8 \times 10^{-3}$. For B mesons we have $\chi_B = 5.5 \times 10^{-7}$. For the detector efficiency of the SHiP experiment we have used the data from simulations obtained from [64]. The resulting contour plots representing the sensitivities of the experiments are given in figure 5.1.

Experiment	POT	l_{dec}	$l_{target-det}$	θ_{min}	θ_{max}	$\Delta\phi$	$\bar{\epsilon}_{\text{det}}$
SHiP	2×10^{20}	50m	50m	0	0.0124	2π	0.48
NA62	1×10^{18}	10m	100m	0	0.0055	2π	1
SHADOWS	5×10^{19}	10m	20m	0.033	0.33	1.79	1

Table 5.1: Parameters of the beam dump experiments at CERN.

You might notice that the detector length of the NA62 experiment is chosen to be smaller than it actually is (10m in stead of 80m), this is because the transverse size of the detector is quite small and particles decaying at the beginning of the detector can escape detection by going into the sides of the detector volume. Also we have chosen the more conservative value for the number of POT of 1×10^{18} in

stead of 5×10^{19} to match it with the sensitivities of NA62 found in the literature which all use the former value.

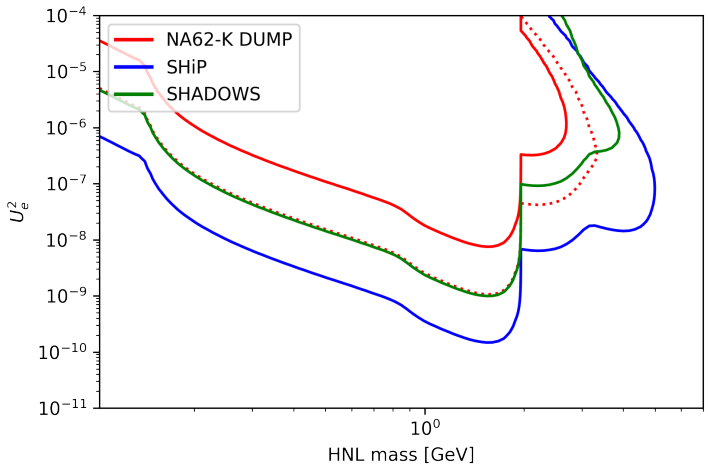

Figure 5.1: Sensitivity of beam dump experiments at CERN for electron dominant mixing ($U_e^2 : U_\mu^2 : U_\tau^2 = 1 : 0 : 0$). The dotted red line is the NA62 DUMP experiment for $N_{POT} = 5 \times 10^{19}$.

5.2 Results for LHC Based Experiments

For the LHC experiments the specifications of the experiments are listed in table 5.2. For all the experiments we do not know the efficiency of the detectors so we will set $\epsilon_{\text{det}} = 1$. The total number of D or B mesons is 4.4×10^{16} and 3×10^{15} respectively.
To match the Codex-b result with the literature we have chosen an integrated luminosity of $300 fb^{-1}$ (solid line in figure 5.2) and compared it to the high luminosity $3000 fb^{-1}$ (dotted).

5.3 Results for DUNE ND

The specifics of the DUNE experiment are given in table 5.4 and the sensitivity is given in figure 5.3. We only consider the decay of D_s mesons since they contribute to the most of the sensitivity curve in the most relevant region. Again we will optimistically set the detector efficiency to unity. Furthermore, due to background

Experiment	l_{dec}	$l_{target-det}$	η_{min}	η_{max}	$\Delta\phi$
MATHUSLA	38.5m	192.5m	0.9	1.6	$\pi/2$
Codex-b	10m	26m	0.13	0.54	0.389
FACET	26m	100m	6.2	7.6	2π
FASER2	10m	480m	6.86	∞	2π

Table 5.2: Relevant parameters for the estimation of the sensitivity region for various experiments at the LHC.

Meson M	B^+	B^0	B^s	B_c^+	D^+	D^0	D_c^+
LHC	0.324	0.324	0.088	2.6×10^{-3}	0.225	0.553	0.105
SHiP	0.417	0.418	0.09	?	0.207	0.632	0.088

Table 5.3: Fragmentation fractions for heavy mesons at LHC ([35] [65] [66]) and SPS ([32][67]) energies.

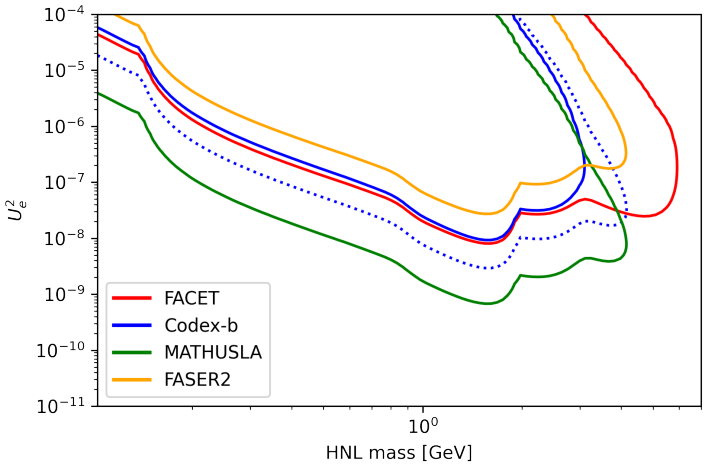

Figure 5.2: Sensitivity of various BSM experiments at LHC for electron dominant mixing ($U_e^2 : U_\mu^2 : U_\tau^2 = 1 : 0 : 0$). The blue solid line is the sensitivity of Codex-b for $300 fb^{-1}$ and the dotted line for $3000 fb^{-1}$.

considerations we must up the level of the contour plot to 85 particles [68]. $N_{POT} = 7.7 \times 10^{21}$

Experiment	N_{D_s}	l_{dec}	$l_{target-det}$	$\Delta\phi$	θ_{max}
DUNE ND	2.2×10^{16}	5m	574m	2π	6 mrad

Table 5.4: Parameters of the DUNE ND experiment for the estimation of its sensitivity to HNLs only taking into account D_s mesons.

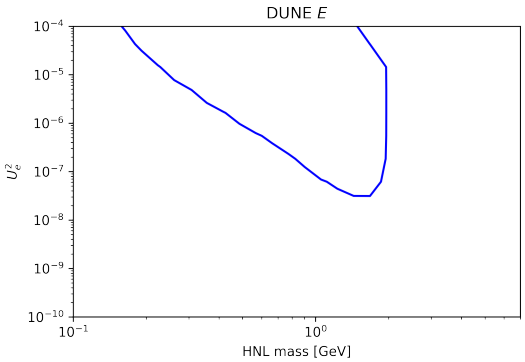

Figure 5.3: Sensitivity for HNLs from D_s mesons at DUNE ND for electron dominant mixing ($U_e^2 : U_\mu^2 : U_\tau^2 = 1 : 0 : 0$).

5.4 Comparison to Literature

We will now overlay our results with previously obtained results and see where they coincide and where they deviate and discuss the significance of these possible differences.

5.4.1 Comparing the extracted beam lines at CERN

See figure 5.4 for the comparison of our results to results from the literature. We see the results are in good agreement especially the results from SHiP [56]. The NA62 results are the most deviant especially in the B meson regime. These discrepancies might be resolved by implementing more detailed kinematical effects.

5.4.2 Comparing results for the LHC based experiments

We see that the results are in fairly good agreement with previous results obtained from the literature and are more close than our beam dump experiments. Especially the MATHUSLA sensitivities and only deviate slightly in the D meson mass region (up to $2GeV$). Also the bump around $1.5GeV$ for the Codex-b experiment is not there but is impossible to get rid of since the general profile of the

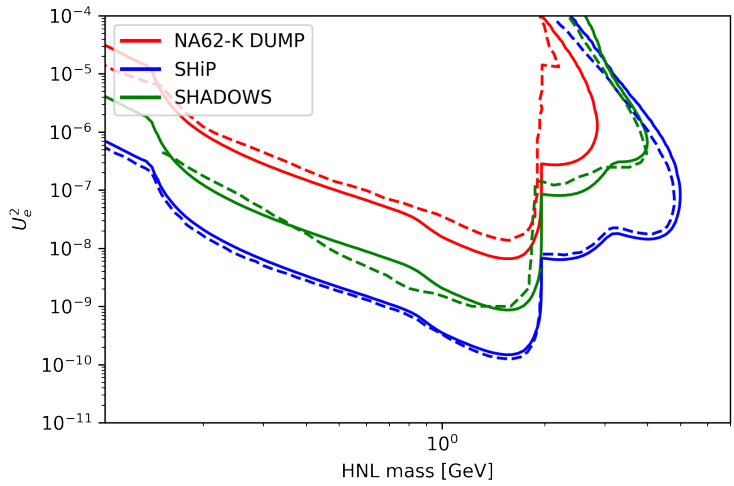

Figure 5.4: Comparison of the previous results with data found in literature. The NA62 result is from [69], SHADOWS from [49] and SHiP from [56].

lower bound is dictated by the various branching ratios in this particular case the branching ratio of the D_s meson.

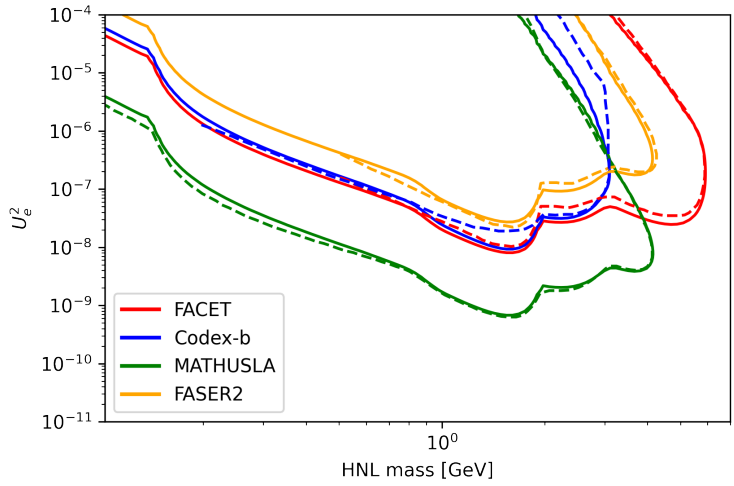

Figure 5.5: Comparison of the sensitivities found in the previous section for LHC based experiments with results from the literature. The FACET result is from [70], Codex-b from [71], MATHUSLA from [56] and FASER2 from [70].

5.4.3 Comparing the DUNE ND result

The result for the DUNE ND experiment matches very well keeping in mind we only consider D_s meson decay while the lower and middle "peaks" are from pions and kaons respectively.

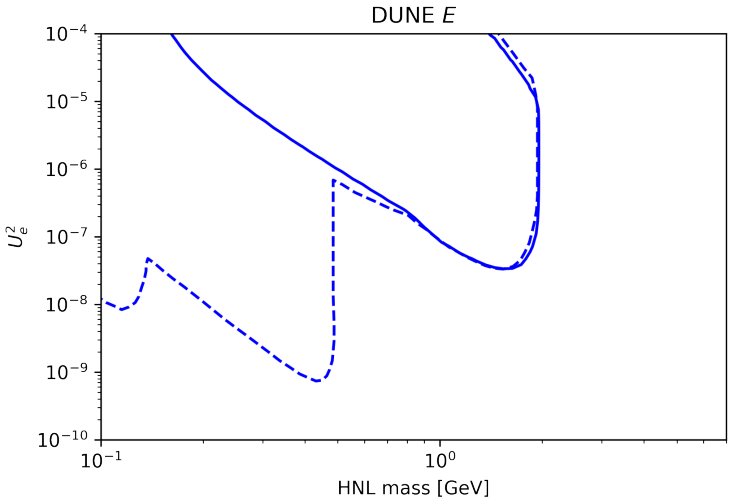

Figure 5.6: Comparison of the DUNE ND sensitivity with the literature [72].

Chapter 6

Conclusions

In this thesis we consistently compared the sensitivity estimates various experiments probing HNL phenomena in particular we looked at Heavy Neutral Leptons. We can draw a number of conclusions:

- The methods outlined and implemented in this thesis produce results that match well with sensitivity estimates from the literature that often utilize more elaborate but error prone methods like Monte Carlo simulations to calculate their sensitivity curves. Our methods are more transparent and could be used to verify these more sophisticated methods.

- Our flexible method is fast and can come in very handy for quick calculations of new estimates in the case of design changes, the proposal of an entirely new experiment or other developments in the field.

- The SHiP experiments shows the highest sensitivity and together with MATHUSLA and FACET covers the parameter space of all the other experiments combined. The superiority of SHiP is predominately evident from its lower bound, which is largely due to its high POT. MATHUSLA has a slight advantage in masses above 2 GeV since the higher energy of the LHC allows for more heavy particles like in our case B mesons. The high maximum mass of the FACET is due to its superior upper bound that extends all the way to the kinematical threshold. The upper bound is determined by the distance of the decay volume from the target to the detector and the gamma factor of the HNL. The upper bound is determined by the fact that particle decay before it can reach the detector, so the closer to the detector the better the upper bound. If the detector is not close, a particle with a high gamma factor might still decay inside the decay volume due to time dilation. We can generally state that $U^2_{max} \propto \gamma_N / l_{target-det}$. The fact that FACET has a

the better upper bound is because it is closer to the detector in the case of FASER and MATHUSLA and is better than Codex-b because FASER covers the forward region which has more particles and with higher gamma factors.

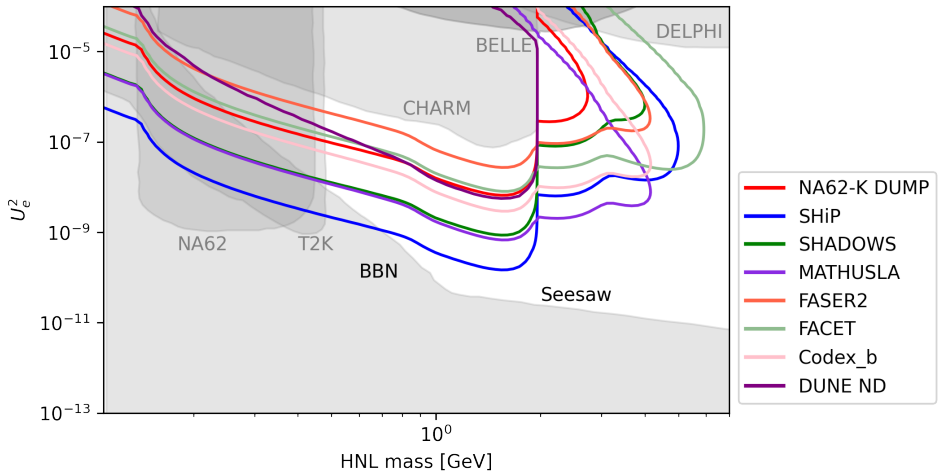

Figure 6.1: Sensitivities of the all the previous results combined together with areas of parameter space already excluded by experiment [73] together with the Seesaw and BBN [74] limits. The Seesaw limit is calculated by the seesaw relation $U_e^2 \sim m_\nu/M_N$, where for active neutrino mass we choose $m_\nu = \sqrt{\Delta m^2_{atm}} \approx 0.05eV$ [33].

Bibliography

[1] B. Pontecorvo, *Mesonium and Antimesonium*, Soviet Journal of Experimental and Theoretical Physics **6**, 429 (1957).

[2] R. Davis Jr, D. S. Harmer, and K. C. Hoffman, *Search for neutrinos from the sun*, Physical Review Letters **20**, 1205 (1968).

[3] E. Kearns, T. Kajita, and Y. Totsuka, *Detecting massive neutrinos*, Scientific American **281**, 64 (1999).

[4] C. S. Wu, E. Ambler, R. W. Hayward, D. D. Hoppes, and R. P. Hudson, *Experimental Test of Parity Conservation in Beta Decay*, Phys. Rev. **105**, 1413 (1957).

[5] S. Weinberg, *Baryon-and lepton-nonconserving processes*, Physical Review Letters **43**, 1566 (1979).

[6] N. Aghanim et al., *Planck 2018 results-VI. Cosmological parameters*, Astronomy & Astrophysics **641**, A6 (2020).

[7] Z. Maki, M. Nakagawa, and S. Sakata, *Remarks on the unified model of elementary particles*, Progress of Theoretical Physics **28**, 870 (1962).

[8] A. G. Cohen, S. L. Glashow, and Z. Ligeti, *Disentangling neutrino oscillations*, Physics Letters B **678**, 191 (2009).

[9] E. K. Akhmedov, *Do charged leptons oscillate?*, Journal of High Energy Physics **2007**, 116 (2007).

[10] A. D. Sakharov, *Violation of CP Invariance, C asymmetry, and baryon asymmetry of the universe*, Pisma Zh. Eksp. Teor. Fiz. **5**, 32 (1967).

[11] G. t Hooft, *Symmetry breaking through Bell-Jackiw anomalies*, Physical Review Letters **37**, 8 (1976).

[12] A. Vaĭnshteĭn, V. I. Zakharov, V. A. Novikov, and M. A. Shifman, *ABC of instantons*, Soviet Physics Uspekhi **25**, 195 (1982).

[13] D. Bödeker, G. D. Moore, and K. Rummukainen, *Hard thermal loops and the sphaleron rate on the lattice*, Nuclear Physics B-Proceedings Supplements **83**, 583 (2000).

[14] M. B. Gavela, P. Hernández, J. Orloff, O. Pene, and C. Quimbay, *Standard model CP-violation and baryon asymmetry (II). Finite temperature*, Nuclear Physics B **430**, 382 (1994).

[15] C. Jarlskog, *Commutator of the quark mass matrices in the standard electroweak model and a measure of maximal CP nonconservation*, Physical Review Letters **55**, 1039 (1985).

[16] V. A. Kuzmin, V. A. Rubakov, and M. E. Shaposhnikov, *On anomalous electroweak baryon-number non-conservation in the early universe*, Physics Letters B **155**, 36 (1985).

[17] K. Kajantie, M. Laine, K. Rummukainen, and M. Shaposhnikov, *Is there a hot electroweak phase transition at m Hâ*^{3}*mW*?, *PhysicalReviewLetters***77**, 2887(1996).

[18] A. V. Zasov, A. S. Saburova, A. V. Khoperskov, and S. A. Khoperskov, Dark matter in galaxies*, Physics-Uspekhi* **60***, 3 (2017).*

[19] F. Bezrukov and D. Gorbunov, Light inflaton hunterâs guide*, Journal of High Energy Physics* **2010***, 1 (2010).*

[20] G. Krnjaic, Probing light thermal dark matter with a Higgs portal mediator*, Physical Review D* **94***, 073009 (2016).*

[21] S. Davidson, E. Nardi, and Y. Nir, Leptogenesis*, Physics Reports* **466***, 105 (2008).*

[22] A. Aguilar et al., Evidence for neutrino oscillations from the observation of ν e appearance in a ν μ beam*, Physical Review D* **64***, 112007 (2001).*

[23] M. Ibe, A. Kusenko, and T. T. Yanagida, Why three generations?*, Physics Letters B* **758***, 365 (2016).*

[24] P. Minkowski, μâ eγ at a rate of one out of 109 muon decays?*, Physics Letters B* **67***, 421 (1977).*

[25] T. Yanagida, Horizontal symmetry and masses of neutrinos*, Progress of Theoretical Physics* **64***, 1103 (1980).*

[26] M. Gell-Mann, P. Ramond, and R. Slansky, Complex spinors and unified theories*, in* Murray Gell-Mann: Selected Papers*, pages 266–272, World Scientific, 2010.*

[27] R. N. Mohapatra and G. Senjanović, Neutrino mass and spontaneous parity nonconservation*, Physical Review Letters* **44***, 912 (1980).*

[28] J. Schechter and J. W. Valle, Neutrino masses in SU (2)â U (1) theories*, Physical Review D* **22***, 2227 (1980).*

[29] J. Schechter and J. W. Valle, Neutrino decay and spontaneous violation of lepton number*, Physical Review D* **25***, 774 (1982).*

[30] M. Dubinin and E. Fedotova, Non-minimal approximation for the type-I see-saw mechanism*, Symmetry* **15***, 679 (2023).*

[31] B. Kyrylo, B. Alexey, K. Juraj, M. Oleksii, R. Oleg, S. Vsevolod, and T. Inar, An allowed window for heavy neutral leptons below the kaon mass*, Journal of High Energy Physics* **2021** *(2021).*

[32] K. Bondarenko, A. Boyarsky, D. Gorbunov, and O. Ruchayskiy, Phenomenology of GeV-scale heavy neutral leptons*, Journal of High Energy Physics* **2018***, 1 (2018).*

[33] S. Alekhin et al., A facility to Search for Hidden Particles at the CERN SPS: the SHiP physics case*, Reports on Progress in Physics* **79***, 124201 (2016).*

[34] E. Graverini, T. Ruf, and E. Van Herwijnen, Mass dependence of branching ratios into HNL for FairShip*, Technical report, 2016.*

[35] R. Aaij et al., Observation of B c+â D 0 K+ decays*, Physical review letters* **118***, 111803 (2017).*

[36] A. M. Abdullahi et al., The present and future status of heavy neutral leptons*, Journal of Physics G: Nuclear and Particle Physics* **50***, 020501 (2023).*

[37] G. Bernardi et al., Search for neutrino decay*, Physics Letters B* **166***, 479 (1986).*

[38] J. Orloff, A. Rozanov, and C. Santoni, Limits on the mixing of tau neutrino to heavy neutrinos*, Physics Letters B* **550***, 8 (2002).*

[39] P. Astier et al., Search for heavy neutrinos mixing with tau neutrinos*, Physics Letters B* **506***, 27 (2001).*

[40] A. Aguilar-Arevalo et al., Improved search for heavy neutrinos in the decay πâ e ν*, Physical Review D* **97***, 072012 (2018).*

[41] E. C. Gil et al., Search for K+ decays to a muon and invisible particles*, Physics Letters B* **816***, 136259 (2021).*

[42] K. Abe et al., Search for heavy neutrinos with the T2K near detector ND280*, Physical Review D* **100***, 052006 (2019).*

[43] P. Abratenko et al., Search for heavy neutral leptons decaying into muon-pion pairs in the MicroBooNE detector*, Physical review D* **101***, 052001 (2020).*

[44] R. Acciarri et al., New Constraints on Tau-Coupled Heavy Neutral Leptons with Masses m N= 280–970 MeV*, Physical review letters* **127***, 121801 (2021).*

[45] S. Collaboration et al., The SHiP experiment at the proposed CERN SPS Beam Dump Facility*, arXiv preprint arXiv:2112.01487 (2021).*

[46] E. C. Gil et al., The Beam and detector of the NA62 experiment at CERN*, Journal of instrumentation* **12***, P05025 (2017).*

[47] E. C. Gil et al., Search for heavy neutral lepton production in K+ decays to positrons*, Physics Letters B* **807***, 135599 (2020).*

[48] N. collaboration et al., The Beam and detector of the NA62 experiment at CERN, 2017.

[49] W. Baldini et al., SHADOWS (Search for Hidden And Dark Objects With the SPS)*, arXiv preprint arXiv:2110.08025 (2021).*

[50] C. Alpigiani et al., Recent progress and next steps for the MATHUSLA LLP detector*, arXiv preprint arXiv:2203.08126 (2022).*

[51] G. Aielli et al., The Road Ahead for CODEX-b*, arXiv preprint arXiv:2203.07316 (2022).*

[52] H. Abreu et al., The FASER detector*, arXiv preprint arXiv:2207.11427 (2022).*

[53] S. Cerci et al., arXiv: FACET: A new long-lived particle detector in the very forward region of the CMS experiment*, Technical report, 2021.*

[54] S. Cerci et al., FACET: a new long-lived particle detector in the very forward region of the CMS experiment*, Journal of High Energy Physics* **2022***, 1 (2022).*

[55] A. A. Abud et al., Deep underground neutrino experiment (DUNE) near detector conceptual design report*, Instruments* **5***, 31 (2021).*

[56] K. Bondarenko, A. Boyarsky, M. Ovchynnikov, and O. Ruchayskiy, Sensitivity of the intensity frontier experiments for neutrino and scalar portals: analytic estimates*, Journal of High Energy Physics* **2019***, 1 (2019).*

[57] M. Anelli et al., A facility to Search for Hidden Particles (SHiP) at the CERN SPS*, arXiv preprint arXiv:1504.04956 (2015).*

[58] S. Collaboration et al., Addendum to Technical Proposal: A facility to Search for Hidden Particles (SHIP) at the CERN SPS*, Technical report, 2015.*

[59] A. Baranov, E. Burnaev, D. Derkach, A. Filatov, N. Klyuchnikov, O. Lantwin, F. Ratnikov, A. Ustyuzhanin, and A. Zaitsev, Optimising the active muon shield for the SHiP experiment at CERN*, in* Journal of Physics: Conference Series*, volume 934, page 012050, IOP Publishing, 2017.*

[60] A. Akmete et al., The active muon shield in the SHiP experiment*, Journal of Instrumentation* **12***, P05011 (2017).*

[61] J. P. Chou, D. Curtin, and H. Lubatti, New detectors to explore the lifetime frontier*, Physics Letters B* **767***, 29 (2017).*

[62] D. Curtin et al., Long-lived particles at the energy frontier: the MATHUSLA physics case*, Reports on progress in physics* **82***, 116201 (2019).*

[63] G. Alves et al., Feynman-x and transverse momentum dependence of D meson production in 250 GeV π, K, and p interactions with nuclei*, Physical Review Letters* **77***, 2392 (1996).*

[64] S. collaboration, HNL sensitivity of SHiP experiment*, 2018.*

[65] R. Aaji et al., Measurement of b hadron production fractions in 7 TeV p p collisions*, Physical Review D* **85***, 032008 (2012).*

[66] F. Kling and S. Trojanowski, Heavy neutral leptons at FASER*, Physical Review D* **97***, 095016 (2018).*

[67] D. Gorbunov and M. Shaposhnikov, How to find neutral leptons of the νMSM?*, Journal of High Energy Physics* **2007***, 015 (2007).*

[68] P. Ballett, T. Boschi, and S. Pascoli, Heavy neutral leptons from low-scale seesaws at the DUNE near detector*, Journal of High Energy Physics* **2020***, 1 (2020).*

[69] M. Drewes, J. Hajer, J. Klaric, and G. Lanfranchi, NA62 sensitivity to heavy neutral leptons in the low scale seesaw model*, Journal of High Energy Physics* **2018** *(2018).*

[70] M. Ovchynnikov, V. Kryshtal, and K. Bondarenko, Sensitivity of the FACET experiment to Heavy Neutral Leptons and Dark Scalars*, Journal of High Energy Physics* **2023***, 1 (2023).*

[71] G. Aielli et al., Expression of interest for the CODEX-b detector*, The European Physical Journal C* **80***, 1 (2020).*

[72] P. Coloma, E. Fernández-Martínez, M. González-López, J. Hernández-García, and Z. Pavlovic, GeV-scale neutrinos: interactions with mesons and DUNE sensitivity*, The European Physical Journal C* **81***, 1 (2021).*

[73] I. Boiarska, A. Boyarsky, O. Mikulenko, and M. Ovchynnikov, Blast from the past: constraints from the CHARM experiment on Heavy Neutral Leptons with tau mixing*, arXiv e-prints , arXiv (2021).*

[74] A. Boyarsky, M. Ovchynnikov, O. Ruchayskiy, and V. Syvolap, Improved big bang nucleosynthesis constraints on heavy neutral leptons*, Physical Review D* **104***, 023517 (2021).*

Acknowledgements

I want to thank my supervisor professor Boyarsky for allowing me to work on one of his projects and my second corrector professor Schalm for agreeing to be my second corrector. Lastly, I want to thank Alex Mikulenko for helping me weekly with various problems surrounding the making of this thesis.